Evaluation of Changes in DRIFT Version 3.7.22

ESR/SRM4689000/003/Rev 1

A report prepared for HSE

01 April 2025

ESR Technology
Engineering, Safety & Risk

Authorisation Sheet

Report Title:	Evaluation of Changes in DRIFT Version 3.7.22
Customer Reference:	
Project Reference:	ESR/SRM4689000
Report Number:	ESR/SRM4689000/003/Rev 1
Issue:	Rev 1
Distribution List:	ESR, HSE

Report Status	Key Changes	Author	Reviewed	Authorised
Rev 0	For Client review	G A Tickle	A Benton	N Ketchell
Rev 1	Changed report title	G A Tickle	N Ketchell	N Ketchell

Executive Summary

DRIFT is a gas dispersion model developed by ESR Technology (ESR). As well as being used by ESR in its consultancy work, DRIFT is also used by the Health and Safety Executive (HSE) as a tool to assist it in performing its regulatory duties and in undertaking its research activities. DRIFT software has also been licenced to third parties.

Rather than re-issue all the existing DRIFT 3 published reports every time a new version of DRIFT is released, it is proportionate to document the testing of new or revised aspects of the model and to undertake comparisons of predictions with those from earlier version(s) for a range of selected cases. These checks are mainly for the purpose of verification testing – to ensure that changes to DRIFT software are behaving as intended and have not had an adverse effect on the previous published validation and verification results.

DRIFT 3.7.19 included improvements over DRIFT 3.6.14 in the modelling of momentum jets, the transition from momentum jet to passive spreading and buoyant lift-off [1]. Detailed comparisons of the results for a wide set of cases (both exemplar and validation) have recently been undertaken by HSE prior to a possible role out of 3.7.19 for wider use within HSE. In general, these comparisons either show little difference between results from 3.7.19 and 3.6.14, or differences that are explainable in terms of the modelling improvements in DRIFT 3.7.19. For a few particular cases, the changes in DRIFT 3.7.19 are found either to have a slightly detrimental effect on agreement with some of the measured values at 100m distance in the Desert Tortoise field trials, or to return misleading hazard ranges for some buoyant cloud scenarios. These cases have been investigated by ESR Technology and some further changes are included DRIFT 3.7.22 to address these issues.

The purpose of this report is to highlight the changes made to the model in version 3.7.22 and to show the impact on the resulting model predictions compared with versions 3.7.19 and 3.6.14. In particular:

- The robustness of the search algorithm used for determining hazard ranges has been improved for the case of buoyant clouds and a bug corrected whereby in the specific circumstance of a transient cloud resulting from a buoyant release DRIFT used zero height, rather than worst case height for calculating concentration contours.

- Compared with DRIFT 3.7.19, results from version 3.7.22 better fit the wall jet data of Davis and Winarto [2] and Rajaratnam [3], whilst a change to the transition from wall jet to wind-blown jets gives improved agreement with the Desert Tortoise data, particularly at 100m distance where the transition algorithm in DRIFT 3.7.19 previously led to concentration predictions exceeding Model Evaluation Criteria developed for evaluating LNG dispersion models.

- Change to ammonia-water interaction coefficients for improved fit to vapour pressure and heat of mixing over a wider range of conditions.

Contents

Tables

Figures

1.0 Introduction

DRIFT is a gas dispersion model developed by ESR Technology (ESR). As well as being used by ESR in its consultancy work, DRIFT is also used by the Health and Safety Executive (HSE) as a tool to assist it in performing its regulatory duties and in undertaking its research activities. DRIFT software has also been licenced to third parties.

Rather than re-issue all the existing DRIFT 3 published reports every time a new version of DRIFT is released, it is proportionate to document the testing of new or revised aspects of the model and to undertake comparisons of predictions with those from earlier version(s) for a range of selected cases. These checks are mainly for the purpose of verification testing – to ensure that changes to DRIFT software are behaving as intended and have not had an adverse effect on the previous published validation and verification results.

DRIFT 3.7.19 included improvements over DRIFT 3.6.14 in the modelling of momentum jets, the transition from momentum jet to passive spreading and buoyant lift-off [1]. Detailed comparisons of the results for a wide set of cases (both exemplar and validation) have recently been undertaken by HSE prior to a possible role out of 3.7.19 for wider use within HSE. In general, these comparisons either show little difference between results from 3.7.19 and 3.6.14, or differences that are explainable in terms of the modelling improvements in DRIFT 3.7.19. For a few particular cases, the changes in DRIFT 3.7.19 are found either to have a slightly detrimental effect on agreement with some of the measured values at 100m distance in the Desert Tortoise field trials, or to return misleading hazard ranges for some buoyant cloud scenarios. These cases have been investigated by ESR Technology and changes included in DRIFT 3.7.21 [4] with some further changes in DRIFT 3.7.22 to address these issues.

The purpose of this report is to highlight the changes made to the model in version 3.7.22 and to show the impact on the resulting model predictions. In particular:

- Improvements in the search algorithm used for determining hazard ranges for the case of buoyant clouds and correction of a bug whereby in the specific circumstance of a transient cloud resulting from a buoyant release DRIFT could use zero height, rather than worst case height for calculating concentration contours.

- Improvements to fitting the wall jet data of Davis and Winarto [2] and Rajaratnam [3], whilst also changing the algorithm for the transition from wall jet to wind-blown jets to give improved agreement with the Desert Tortoise data, particularly at 100m distance where the transition algorithm in DRIFT 3.7.19 previously led to concentration predictions exceeding Model Evaluation Criteria developed for evaluating LNG dispersion models.

- Change to ammonia-water interaction coefficients for improved fit to vapour pressure and heat of mixing over a wider range of conditions.

2.0 Changes included in DRIFT 3.7.22

2.1 Search algorithm for hazard ranges

Some exemplar test cases run by HSE showed that DRIFT 3.7.19 sometimes returned negative hazard ranges and inconsistent contour plots. Investigation of these cases has shown the negative hazard ranges to result from the search algorithm not being sufficiently robust in the circumstance that the cloud radius decreases between time steps. The circumstance of the cloud radius being predicted to decrease represents an unusual situation, but it can occur in DRIFT in the circumstance of a buoyant release from an area source (or equivalent imported from a GASP run). The search algorithm in DRIFT 3.7.19 wrongly interpreted this situation as the cloud moving in the opposite direction to the wind and hence erroneously reported the hazard ranges. In DRIFT 3.7.21 the search algorithm was modified to avoid interpreting the cloud as moving backwards in this circumstance.

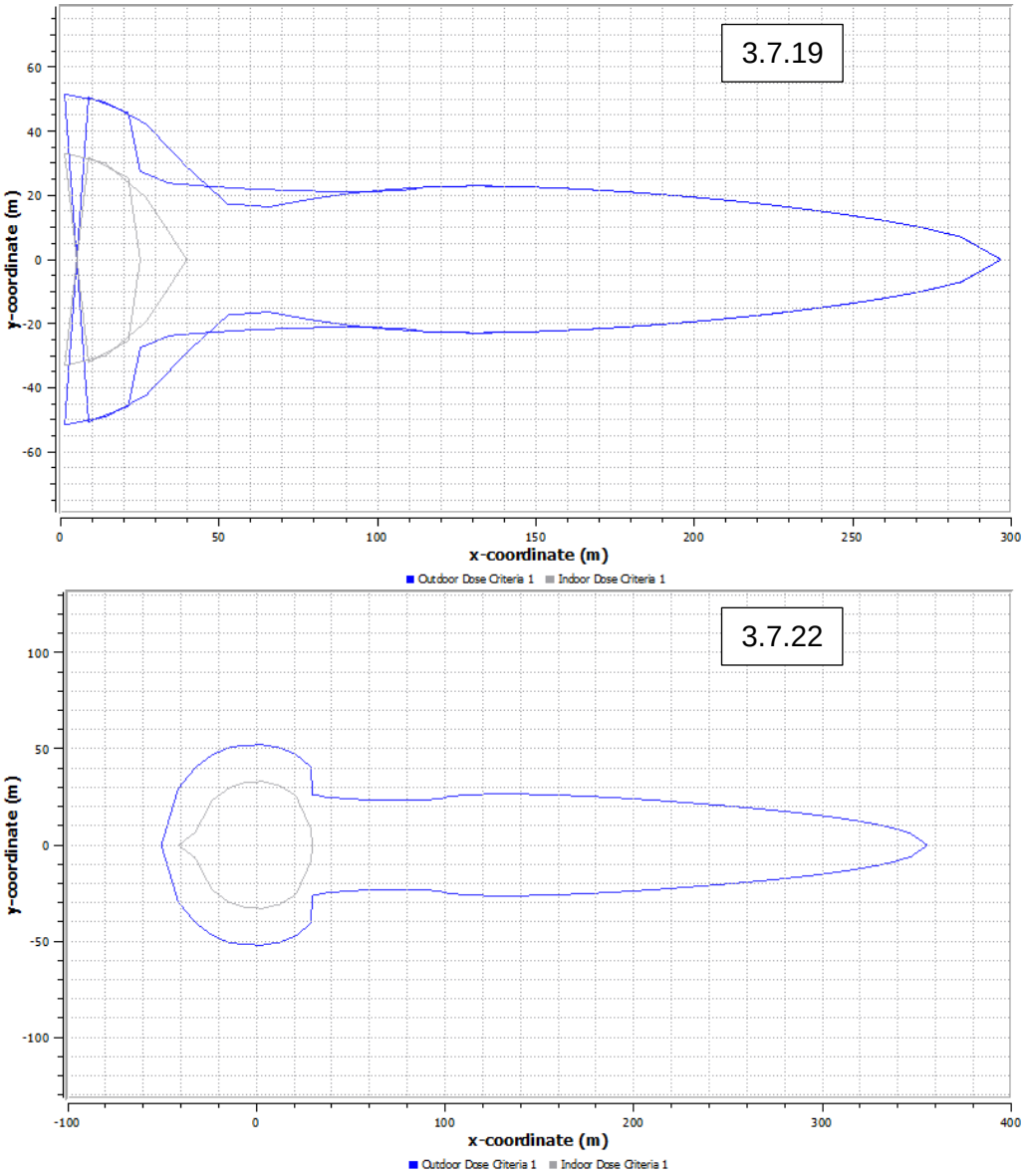

Figure 2-1 Toxic SLOT plan view contours (blue=outdoors, grey=indoors) for scenario NH3_F2.4_42 (pool). Wind blows from low to high x.

As an example, Figure 2-1 and Table 2-1 show a comparison of predicted SLOT contours and hazard ranges for dispersion from the vaporisation of an ammonia pool as reported by DRIFT's graphical

user interface (GUI). The DRIFT 3.7.19 contour plot does not show the extent upwind, and the reported upwind hazard range is incorrectly determined. This bug was fixed in DRIFT 3.7.21 [4]. DRIFT 3.7.22 shows the upwind portion of the contours as well as the downwind and the reported hazard ranges are consistent with these contours once account is taken for the difference between curvilinear centreline and horizontal plan view distances - the contours are plan view and show the horizontal extents, whereas the hazard ranges in Table 2-1 are curvilinear distances measured along the centreline trajectory which are generally longer due to the additional vertical travel associated with buoyant rise.

Table 2-1 Outdoors toxic SLOT hazards ranges for scenario NH3_F2.4_42 (pool)

	3.7.19	**3.7.22**
Upwind distance to SLOT (m)	296	50
Downwind distance to SLOT (m)	345	399
Maximum half width to SLOT (m)	52	52
Downwind distance to maximum half width (m)	0	0

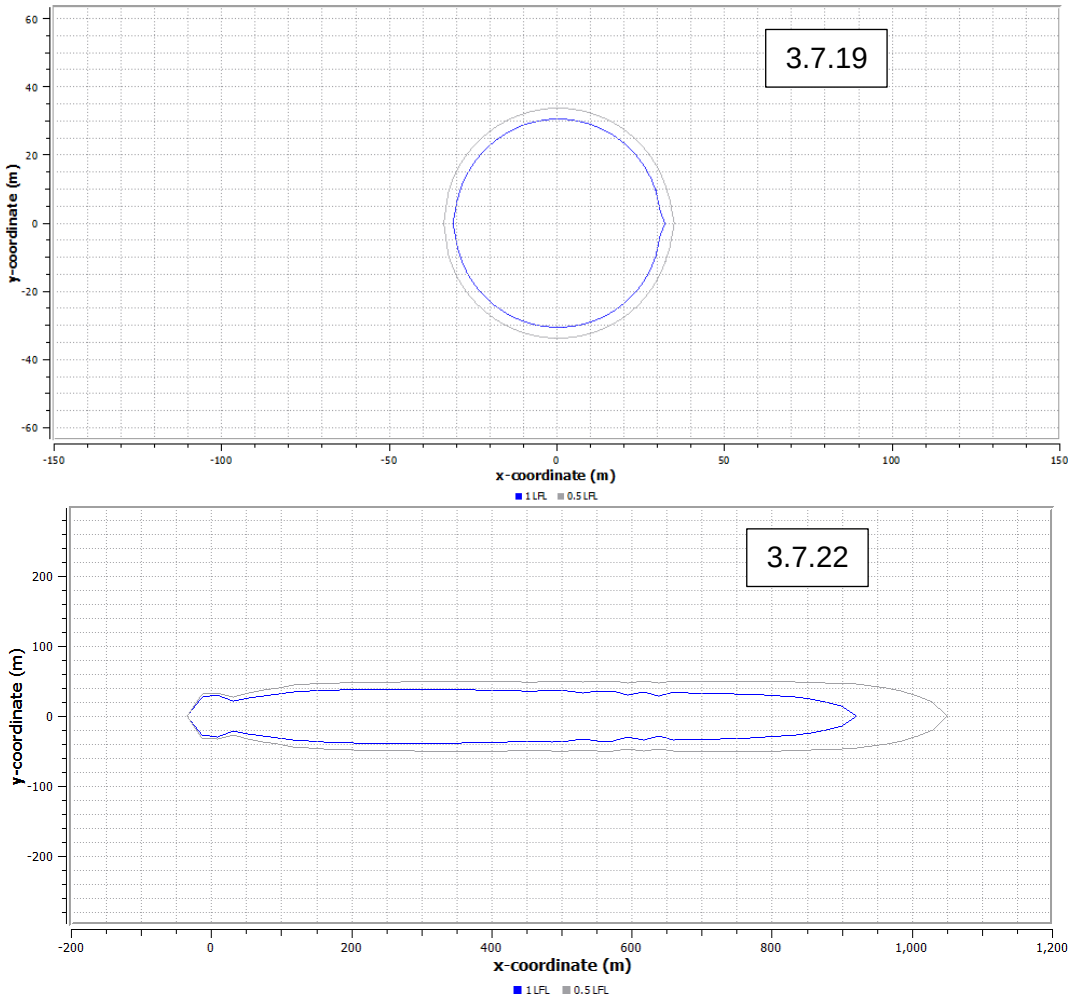

Figure 2-2 Flammable plan view contours from buoyant transient cloud (3 te hydrogen released over 11s in F2 conditions)

Whilst investigating this, another bug was identified whereby in the circumstance of there being no steady state dispersion established over the duration of the release, the resulting transient cloud hazard ranges and contours were always being calculated at ground level (corresponding to zero height) irrespective of the requested height (worst case or specified height). This could result in a

large difference between the results from a buoyant cloud depending upon whether a steady source is established or not. This additional bug has been fixed in DRIFT 3.7.21 and later. As an example, Figure 2-2 shows a comparison between results from DRIFT 3.7.19 and DRIFT 3.7.22 for a buoyant transient release of hydrogen from an area source (pool). In the case of DRIFT 3.7.19, because it is contouring at zero height, only the contour corresponding to the pool extent is shown, whereas the contours from DRIFT 3.7.22 show the full predicted extent of the cloud. Figure 2-3 shows the side view contours from DRIFT 3.7.22 – it can be seen that the buoyant cloud is elevated and trapped below the atmospheric boundary layer mixing height at 100m. DRIFT predicts low rates of dilution for such trapped elevated clouds due to the low level of atmospheric turbulence at high elevation. Such elevated clouds require careful interpretation in terms of whether they represent a hazard at lower elevations. It is also possible that for elevated clouds that extend over a significant fraction of the boundary layer, the true mixing of the cloud is underestimated since DRIFT's elevated model is based upon centreline values only and turbulence will be higher at lower heights.

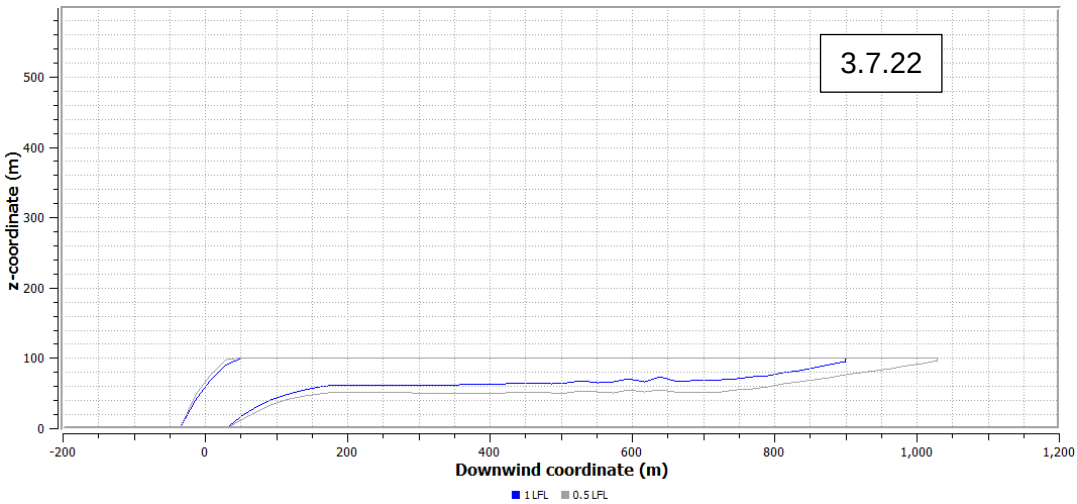

Figure 2-3 Flammable side view contours from buoyant transient cloud (3 te hydrogen released over 11s in F2 conditions)

The above described bugs existed in DRIFT 3.7.19 and also in previous versions including 3.6.x but they were more likely to occur in 3.7.19 due to a greater tendency for buoyant lift-off in 3.7.19 as a result of its improved fit to URAHFREP wind-tunnel data for dispersion from buoyant area sources [1].

2.2 Wall jet modelling

As described in [1], DRIFT 3.7.19 included changes to entrainment and spreading to improve, as compared with 3.6.x, the agreement of predictions with wall jet data. It was noted in [1], that although improved compared with 3.6.x, there was scope to get better agreement for the lateral and vertical spreading rates compared with Davis and Winarto data [2], particularly for the lowest height release (h/D=0.5, where h is the release height and D is the release diameter).

The wall jet entrainment and spreading models have been revised in DRIFT 3.7.22 with the aim of better fitting the wall jet behaviour of Davis and Winarto, whilst maintaining the broad agreement with centreline velocity decay data of Rajaratnam and not unduly increasing concentration predictions for the Desert Tortoise field trials.

In DRIFT entrainment is modelled as a sum of contributions from top entrainment and edge entrainment terms. In the continuous model the rate of entrainment of ambient air is given by:

$$\frac{d\mu_a}{ds} = n_a[2Wu_T + 2Hu_E]$$

where μ_a is the molar flux of air in the plume, $n_a$is the number of moles of air per unit volume in the atmosphere, s is the distance along the trajectory of the centreline, W is the half-width of the plume and H is the depth of the plume. u_T and u_E are top and edge entrainment velocities. Here we shall consider only the grounded model where the plume is at zero height, denoted below by subscript, g.

In DRIFT 3.7.22 the top and edge entrainment velocities are simply given by the maximum of different mixing mechanisms:

$$u_{Tg} = \max\left[u_{T,passive}, u_{Tg,jet}\right]\phi_T$$
$$u_{Eg} = \max\left[u_{E,grav}, u_{E,passive}, u_{Eg,jet}\right]$$

where $u_{T,passive}$ and $u_{E,passive}$ are the top and edge entrainment velocities during passive dispersion, $u_{E,grav}$ is the edge entrainment velocity due to gravity spreading, $u_{Tg,jet}$ and $u_{Eg,jet}$ are the top and edge entrainment velocities due to the wall jet.

The function ϕ_T represents the suppression (or enhancement) of vertical mixing due to the stable stratification of the dense cloud (or enhanced vertical mixing for a buoyant cloud) which is a function of the cloud Richardson number:

$$\phi_T = \phi_T(Ri_{*c})$$

$$Ri_{*c} = \frac{g'H}{{u_{*c}}^2}$$

where $g' = g \cdot (\rho/\rho_a - 1)$ is the reduced gravitational acceleration and u_{*c} is the friction velocity for the cloud which is taken as the maximum of the atmospheric and jet friction velocities:

$$u_{*c} = \max\left[u_{*}.u_{*,jet}\right]$$

In DRIFT 3.7.19 ϕ_T simply used a Richardson number based upon the atmospheric friction velocity.

In DRIFT 3.7.22 the wall jet entrainment velocities are given by:

$$u_{Tg,jet} = u_{Eg,jet} = f_{1g}\sqrt{\frac{\rho}{\rho_a}}\alpha_{jet}|\boldsymbol{U} - \boldsymbol{U}_a|$$

Where ρ is the jet centreline density, ρ_a is the ambient air density, $\boldsymbol{U}$ is the bulk jet velocity and $\boldsymbol{U}_a$ is the ambient wind speed at the cloud centroid height. The entrainment coefficient α_{jet} is taken to have a constant value and f_{1g} is an empirical function to suppress the initial mixing at the jet centreline. It is found that a reasonable representation of the asymptotic centreline velocity decay is obtained by setting α_{jet} = 0.05 with

$$f_{1g} = \min[1, 0.3\mu/\mu_0]$$

where μ_0 is the initial molar flux in the jet and μ is the total molar flux (increasing with distance). Figure 2-4 shows a comparison of the resulting DRIFT model predictions with the wall jet data published by Rajaratnam [3].

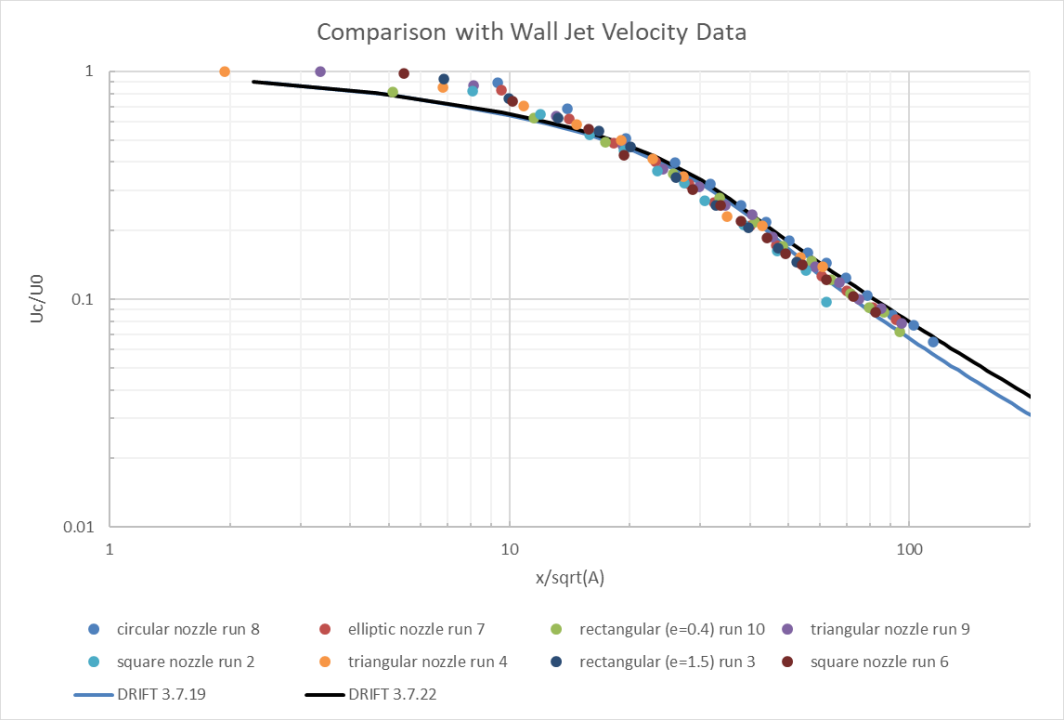

Figure 2-4 Decay of centreline velocity in DRIFT 3.7.22 compared with wall jet data of Rajaratnam [3]. x is the centreline distance from the nozzle exit and A is the cross-sectional area of the nozzle.

In a similar manner, the lateral spreading rate of the ground level plume is taken to be the maximum of the spreading rate for different regimes:

$$\frac{dW}{ds} = \max\left[\left(1 - f_{jet}\right)\beta_{grav} + f_{jet}\beta_{passive}, \beta_{jet}\right]$$

Where β_{grav} is the lateral spreading rate due to gravity, $\beta_{passive}$ the spreading rate of a passive plume and β_{jet} the spreading rate of the wall jet. After an initial adjustment distance, wall jets in still air are observed to spread linearly with distance at a constant rate. In DRIFT 3.7.22 the following empirical expression is used:

$$\beta_{jet} = f_{2g} f_{3g} \beta_{jet\infty}$$

where:

$$f_{2g} = \min\left[1.0, f_{jet}\right]$$

$$f_{3g} = \min[1, 0.3U_0/U_C]$$

$$f_{jet} = \frac{u_{Eg,jet}H + u_{Tg,jet}W}{u_{Eg}H + u_{Tg}W}$$

$$\beta_{jet\infty} = 0.27\,\Gamma\left(1 + \frac{1}{w}\right)/(\ln(2))^{1/w}$$

U_0 is the initial velocity (after expansion to atmospheric pressure) and U_c is the centreline velocity which decreases with distance. f_{3g} represents an initial suppression of spreading due to the zone of flow development where the profiles adjust from uniform at the exit to Gaussian in the jet. The purpose of f_{2g} is to ensure transition from linear wall jet spreading to either gravity or passive

spreading when the entrainment rate of air into the plume is no longer dominated by jet entrainment. The effect of this is further discussed in Section 2.4. The term $\Gamma\left(1+\frac{1}{w}\right)/(\ln(2))^{1/w}$ in $\beta_{jet\infty}$ is a profile dependent correction to the observed asymptotic lateral spreading rate (0.27) of the half-width to ½ times the centreline velocity; Γ is the gamma function and w is the lateral profile shape parameter ($w = 2$ corresponds to a Gaussian shaped profile and $w \to \infty$ gives a uniform profile).

Figure 2-5 to Figure 2-10 show comparisons of DRIFT's predictions for centreline velocity U_c and horizontal L_y and vertical L_z length scales (both to 1/2 the centreline velocity) with Davis and Winarto wall jet data. Predictions are shown for DRIFT versions 3.6.14, 3.7.19 and 3.7.22. Overall DRIFT 3.7.22 best captures both the observed centreline velocity and lateral growth.

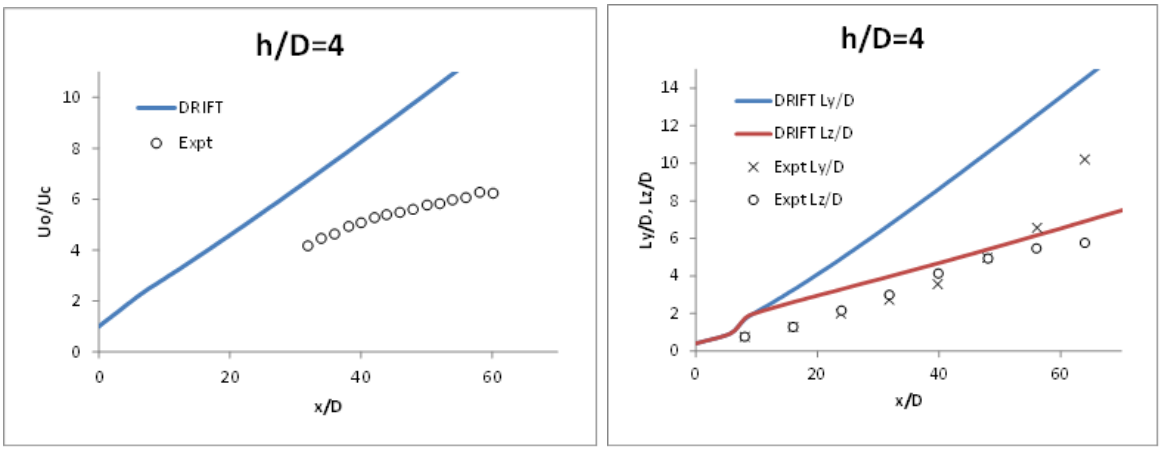

Figure 2-5 Velocity predictions of DRIFT 3.6.14 for h/D=4 compared with Davis and Winarto data [2].

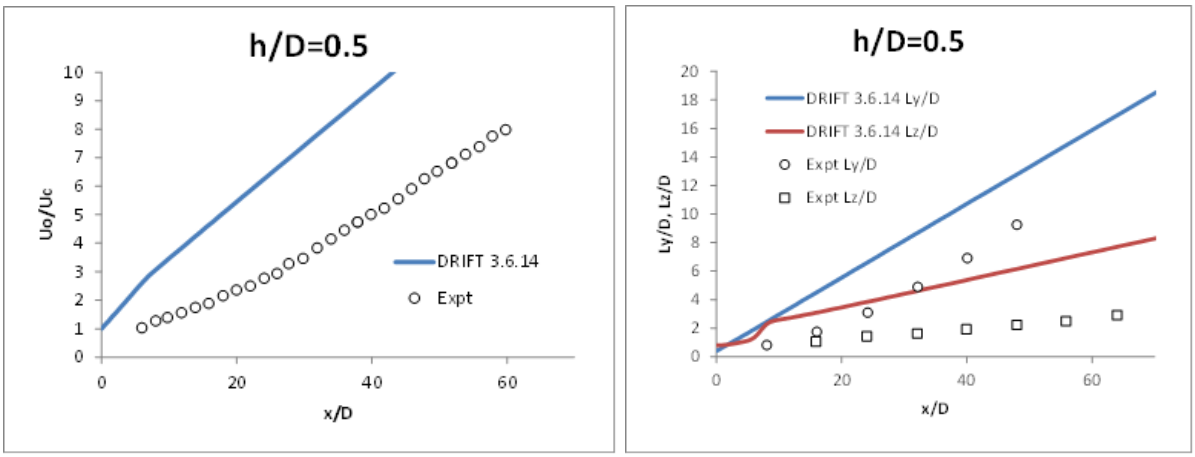

Figure 2-6 Velocity predictions of DRIFT 3.6.14 for h/D=0.5 compared with Davis and Winarto data [2].

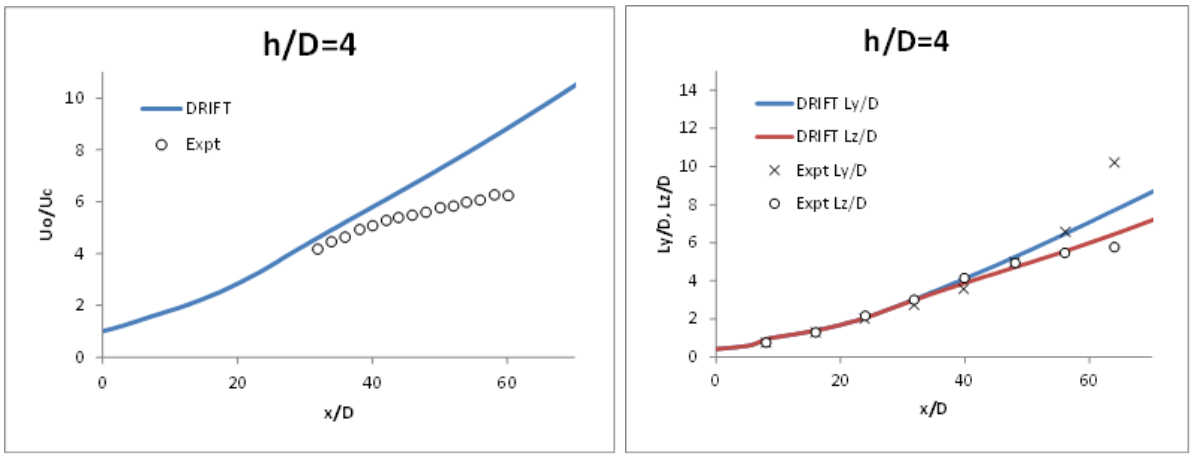

Figure 2-7 Velocity predictions of DRIFT 3.7.19 for h/D=4 compared with Davis and Winarto data [2].

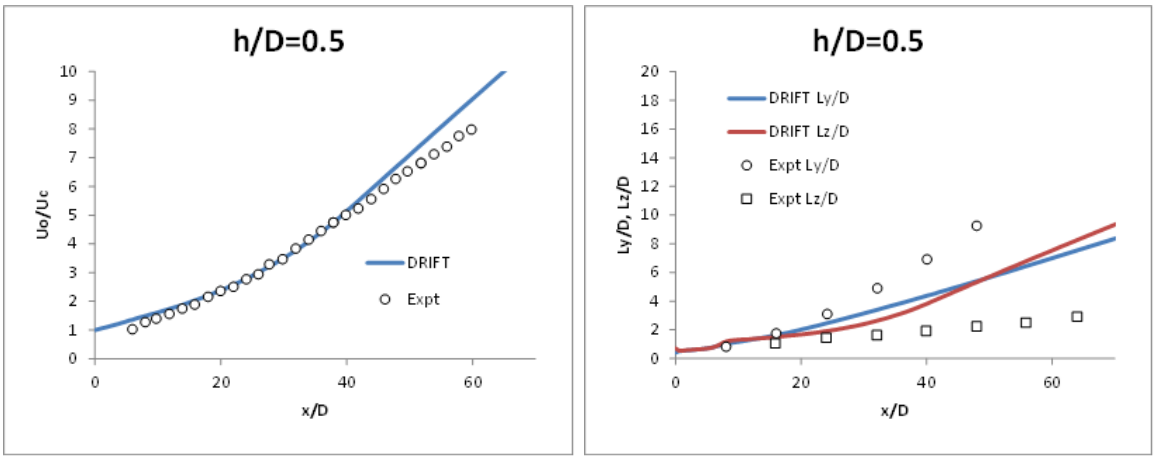

Figure 2-8 Velocity predictions of DRIFT 3.7.19 for h/D=0.5 compared with Davis and Winarto data [2].

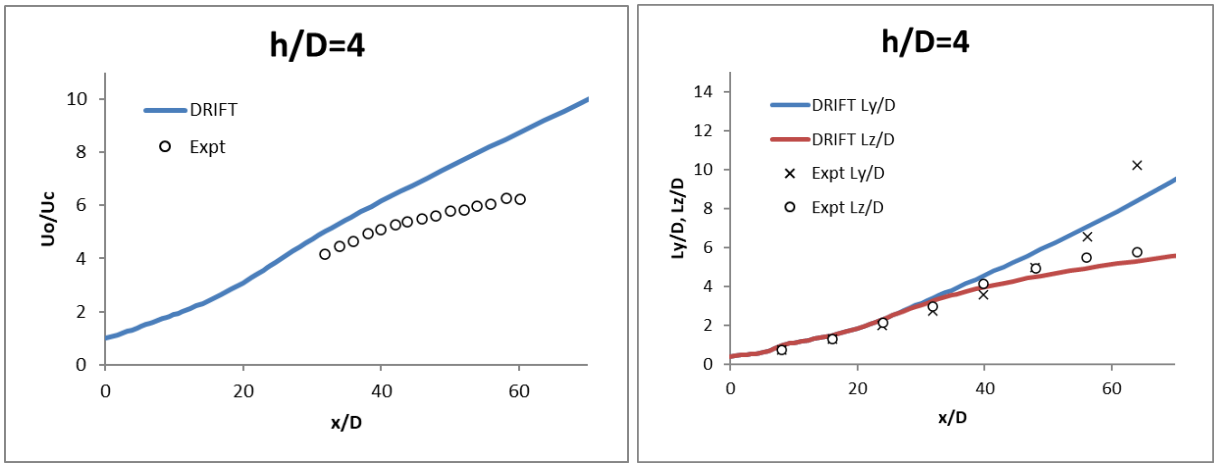

Figure 2-9 Velocity predictions of DRIFT 3.7.22 for h/D=4 compared with Davis and Winarto data [2].

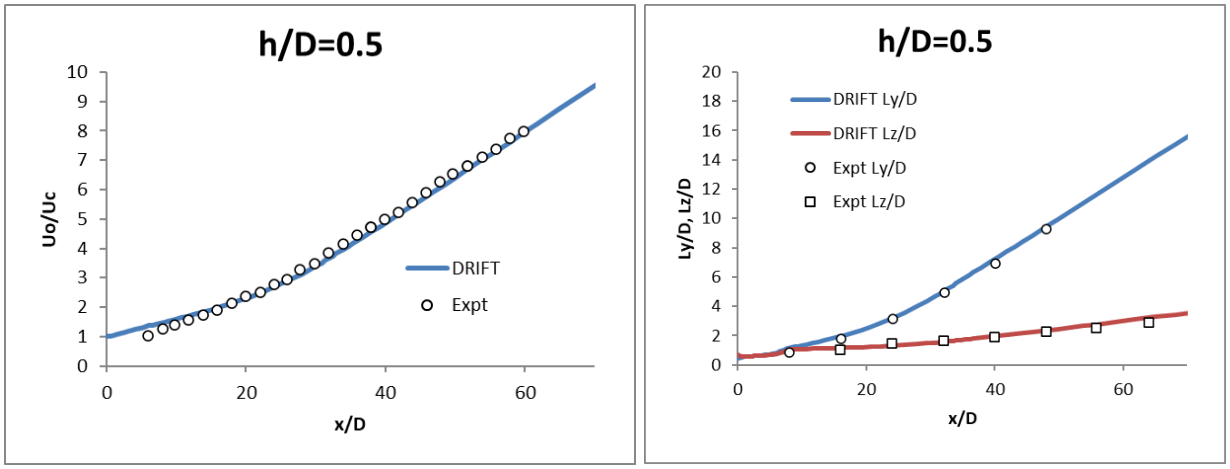

Figure 2-10 Velocity predictions of DRIFT 3.7.22 for h/D=0.5 compared with Davis and Winarto data [2].

2.3 Desert Tortoise field trials

Desert Tortoise field trials are large scale two-phase jet releases of ammonia in relatively dry desert conditions. DRIFT version 3.7.19 predictions for three of the Desert Tortoise trials (DT1, DT2 and DT3) have been submitted to a model inter-comparison exercise undertaken as part of the Jack Rabbit III project. The DRIFT 3.7.19 predictions for these three Desert Tortoise trials were found to consistently overpredict the average concentrations and also to lie marginally outside of acceptance criteria. DRIFT 3.6.14 predictions for the same trials were found to lie marginally within acceptance criteria. An initial investigation of these differences suggested that they were in part due to changes in wall jet modelling included in DRIFT 3.7.19, and in particular the method used to transition from wall jet mixing and spreading to wind-blown dispersion. An aim in the 'recalibration' against wall jet data in 3.7.21 and DRIFT 3.7.22 was to better match the spreading and decay for wall jets and to seek a method of transition from wall jet to wind-blown jet that simultaneously better matches the Desert Tortoise trial measurements.

DRIFT predictions for Desert Tortoise trials 1-4 have been compared with the measured field values using both DRIFT 3.7.19 and DRIFT 3.7.22. Table 2-2 shows a comparison of the Statistical Performance Measures (SPMs) for both peak and time-averaged concentrations. It can be seen that DRIFT 3.7.22 produces overall predictions that more closely match the measurements. The geometric mean bias of less than one shows a tendency for DRIFT to overpredict the measurements, particularly when compared with averaged concentrations, although most predictions are within a factor of 2 of the measured values.

Table 2-2 Comparison of Statistical Performance Measures for Concentration Predictions of Desert Tortoise Field Trails

		DRIFT 3.7.19		DRIFT 3.7.22	
Statistical Performance Measure	Abbrev.	peak	averaged	Peak	averaged
Mean Relative Bias	MRB	-0.33	-0.59	0.06	-0.26
Mean Relative Square Error	MRSE	0.15	0.40	0.06	0.13
Fraction of predictions within a factor of two of measurements	FAC2	0.88	0.63	1.00	1.00
Geometric Mean Bias	MG	0.71	0.54	1.06	0.76
Geometric Variance	VG	1.18	1.55	1.06	1.14

Figure 2-11 shows a plot of the geometric mean variance (VG) against the geometric mean bias (MG) for the concentration predictions of these trials. Perfect agreement with measured values would lie at (1,1) on this plot. The vertical lines of MG=0.5 and MG=2 represent factor of two overprediction and underprediction about the mean. The lines $VG = \exp(\ln MG)^2$ define the minimum possible values for VG and the red rectangle shows acceptability criteria given in [5]. This plot shows that the changes included in version 3.7.22 bring DRIFT predictions within the acceptance criteria given in [5]. Interestingly for these Desert Tortoise trials DRIFT gives much better agreement with peak (short time averaged) measured concentrations than for the time-averaged concentrations and the greater overprediction for the time-averaged values. Looking in detail at the predictions for each trial, the greatest overprediction is for trial DT1 which has the shortest averaging time (80s). This may indicate that the lateral meander time-averaging model might not fully be accounting for the variation observed in these trials particularly for trial DT1.

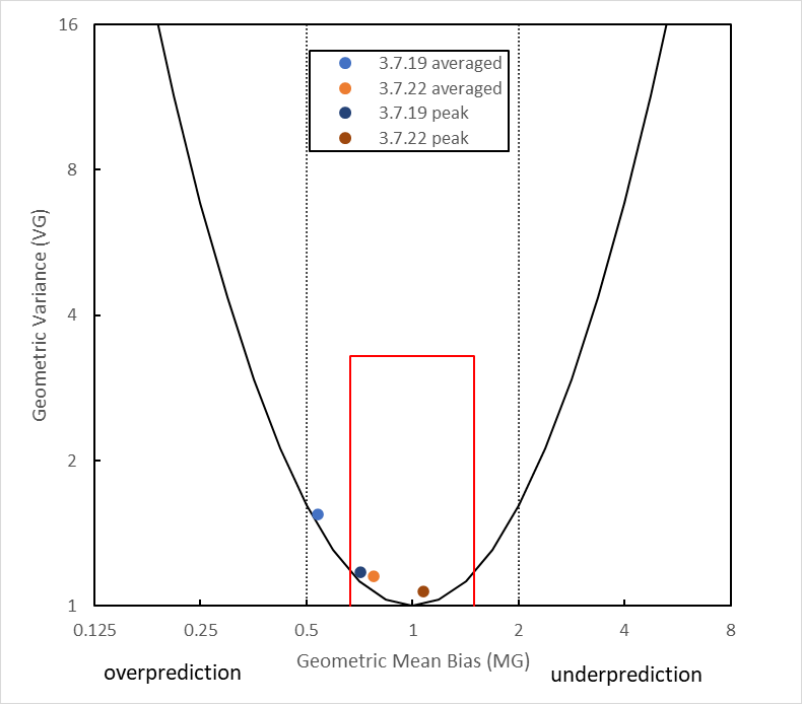

Figure 2-11 Geometric Variance vs Geometric Mean Bias for Desert Tortoise Trials

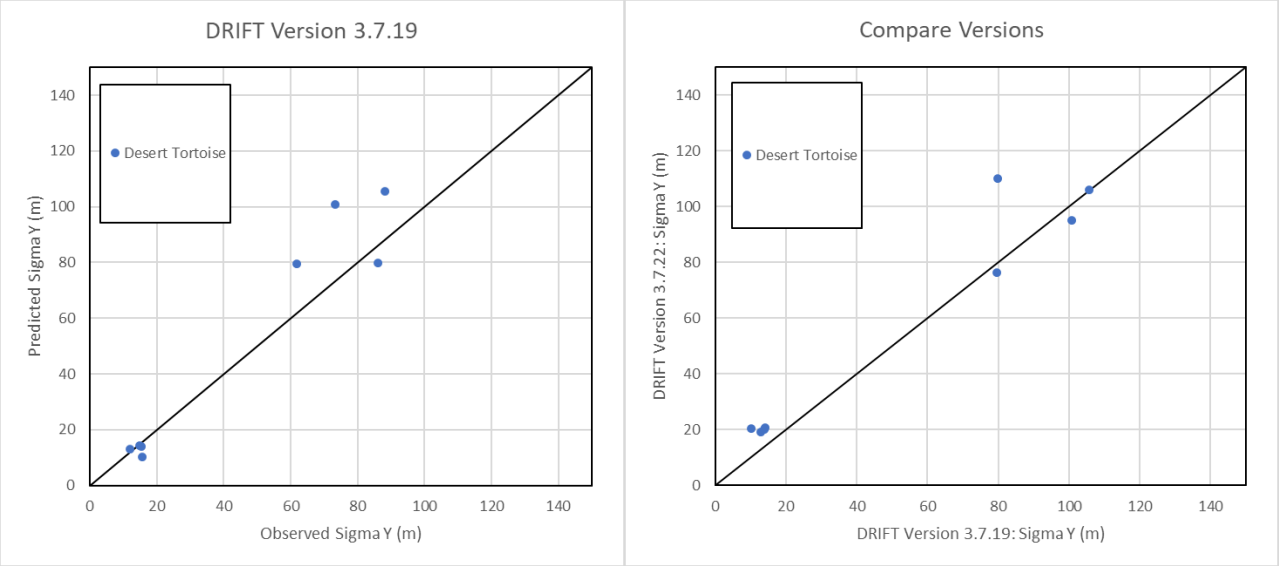

Figure 2-12 Predicted vs observed cloud widths (sigma-y) for Desert Tortoise Trials

Figure 2-12 shows plots of predicted against observed cloud widths (sigma-y) for DRIFT 3.7.19 and DRIFT 3.7.22. DRIFT 3.7.22 generally shows closer agreement between predicted and measured values.

2.4 Transition from wall jet to passive spreading

As explained in [1] a problem in DRIFT versions prior to 3.7.15 was that DRIFT could hang on to jet spreading and dilution far downstream, even when the jet had slowed to very close to the wind speed. The fix in 3.7.15 was to include an empirical function to kill off jet spreading and dilution when the magnitude of the velocity excess above the ambient wind velocity normalised by the jet speed dropped below unity. Although this ensures the correct behaviour in the passive limit, it appears that this transition algorithm is a contributory factor to the overprediction of the Desert Tortoise trials in DRIFT 3.7.19. The alternative transition approach described in Section 2.2 of this report gives rise to a slower transition in DRIFT 3.7.22, based upon the fraction of the entrainment rate that is associated with jet entrainment. Another difference in DRIFT 3.7.22 is that the top entrainment factor ϕ_T now applies also to the jet entrainment phase and uses a Richardson number that includes jet friction velocity.

Figure 2-13 shows the predicted centreline concentration decay with distance for a very large steady continuous release in F2 weather conditions. Since the steady continuous model is used there is no inclusion of along wind diffusion which would act to mask differences in the far field. For this case beyond 1 km distance DRIFT 3.7.19 predictions are very close to DRIFT 2 predictions which do not account for any jet mixing. It is seen that the new approach in DRIFT 3.7.22 gives centreline concentrations similar to PHAST 7.2 and 8.9 (these PHAST runs are for a large non-decaying release rate which is maintained for a long duration such that along wind diffusion can be ignored). DRIFT 3.6.14 predicts lower concentrations over most of this distance range, likely due to the model holding on to jet spreading and the lack of entrainment suppression in the near field of the wall jet.

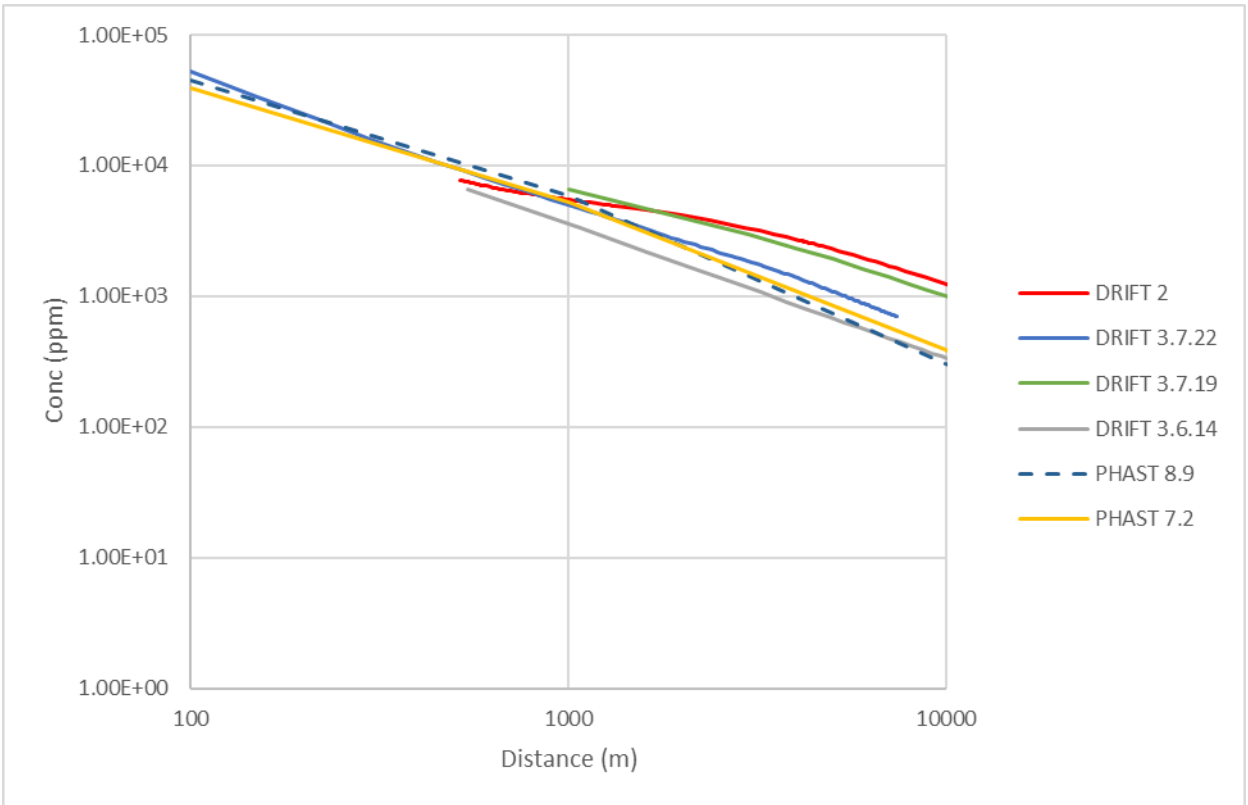

Figure 2-13 Comparison of transition from wall jet to passive spreading for a very large steady continuous release in F2 conditions.

2.5 Ammonia-water interactions

DRIFT 3.7.21 and 3.7.22 incorporate revised binary interaction coefficients to improve the fit to experimental data across a wider range of conditions than previously. DRIFT uses a binary interaction model due to Wheatley [6]. Revised coefficients have been derived by fitting to a thermodynamically self-consistent correlation published by Tillner-Rothe and Friend [7]. Fitting to the Tillner-Roth and Friend correlation is preferred to the original fit of Wheatley since Tillner-Roth and Friend includes newer high-quality data over a wider range of temperatures and compositions.

The revised binary interaction coefficients in DRIFT 3.7.21 and 3.7.22 are:

$w_A = 2100$
$w_B = 6.8106$
$r_A = 0.0$
$r_B = -0.3812$

which replace the previous values due to Wheatley [6]:

$w_A = -185$
$w_B = -0.34$
$r_A = -14$
$r_B = -14$

The definitions of w_A, w_B, r_A and r_B are given in [6].

Figure 2-14 shows the predicted (curves) bubble point pressure of the mixture compared with spot values from the Tillner-Roth and Friend correlation as a function of mole fraction of ammonia (NH_3) in the mixture. Values are given at temperatures ranging from -30 °C up to 40 °C. The solid lines and dots are the bubble point pressure as a function of the mole fraction (x) of ammonia in the liquid phase, and the dashed lines and crosses are the bubble point pressure as a function of the mole fraction (y) of ammonia in the vapour phase. The upper plot in Figure 2-14 shows the predictions using Wheatley's original coefficients and the lower plot shows the predictions using the newly fitted coefficients in DRIFT 3.7.21 and 3.7.22. The new fit shows slightly improved agreement with the Tillner-Roth Friend correlation particularly at lower mole fractions of ammonia.

Figure 2-15 shows the predicted heat of mixing compared with spot values from the Tillner-Roth and Friend correlation. DRIFT's predicted heat of mixing is independent of temperature, whereas the Tillner-Roth and Friend correlation shows a very weak temperature dependence. The new fit shows a symmetrical dependence around 0.5 mole fraction and a greater maximum heat of mixing than the original Wheatley fit.

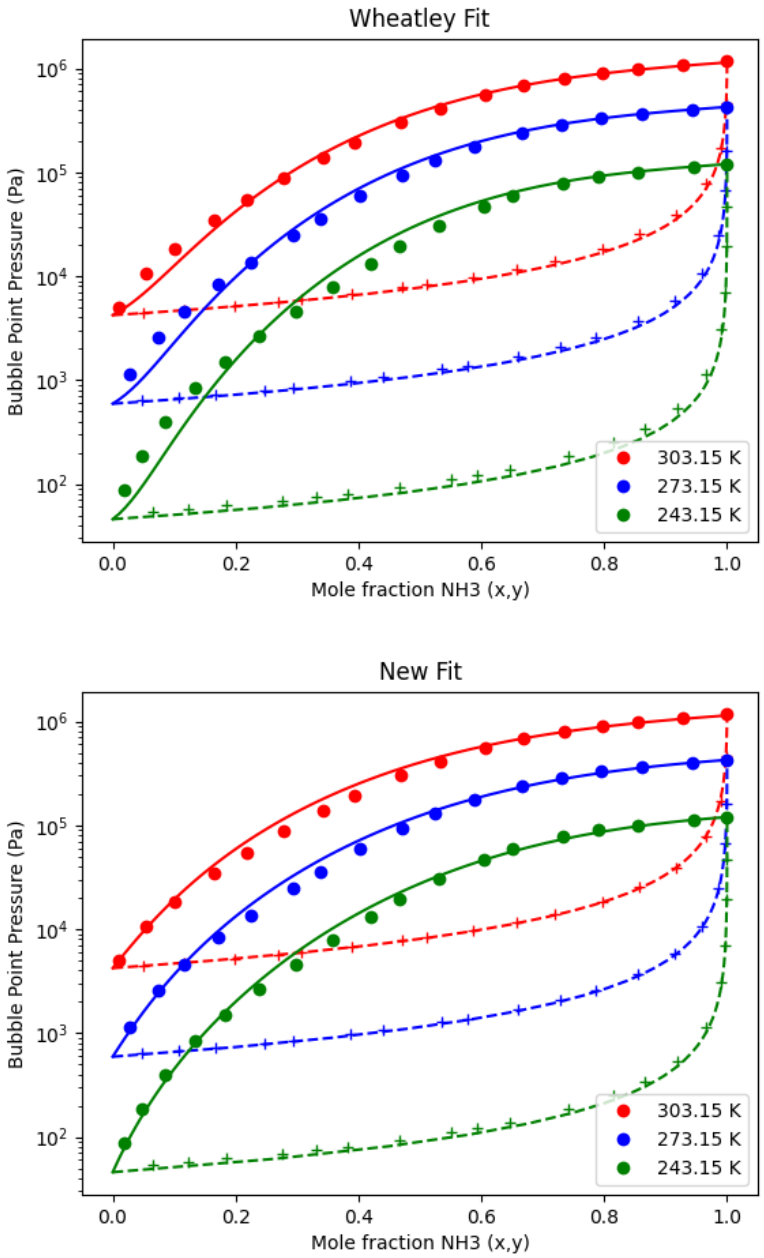

Figure 2-14 Comparisons of predicted bubble point pressure for ammonia-water liquid mixtures. Curves are model predictions and symbols are Tillner-Roth Friend correlation.

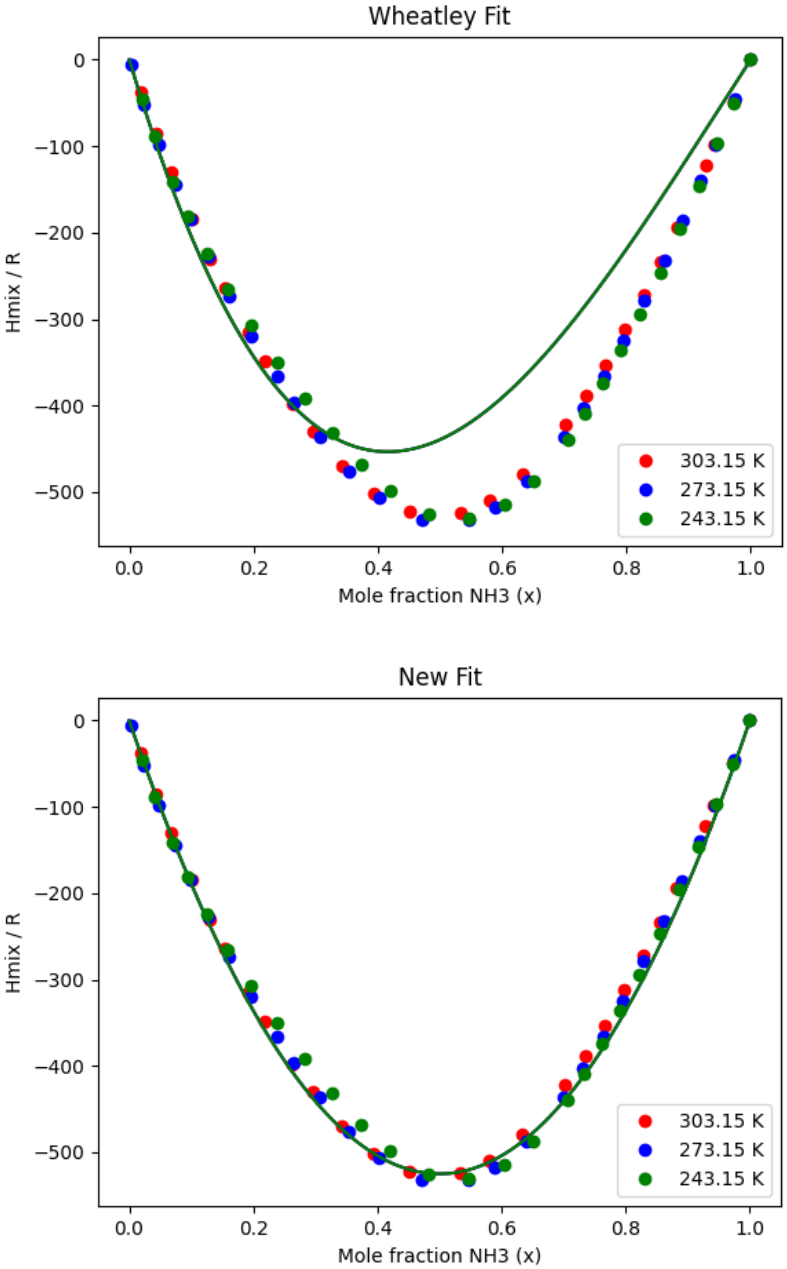

Figure 2-15 Comparisons of predicted heat of mixing (Hmix) for ammonia-water liquid mixtures. Curves are model predictions and symbols are Tillner-Roth Friend correlation. R is the universal molar gas constant.

3.0 Other Checks

3.1 Momentum jets

One of the main changes in moving from DRIFT 3.6.x to 3.7.x is testing and improvement of the momentum jet modelling in DRIFT. DRIFT 3.6.x already included a momentum jet model, but testing of the jet model was limited, and considered to be less extensive than the testing previously undertaken for the standalone jet model EJECT. Testing relating different aspects of the jet model are summarised below.

3.1.1 Comparison with JINX

JINX is an implementation of the gas jet model of Cleaver and Edwards [8]. Predictions of DRIFT 3.7.22 have been compared with those of JINX Version 2.1.2 (used under licence by ESR Technology) for the following cases:

- 100 bara methane from 50 mm hole
- 10 bara methane from 50 mm hole

The releases are horizontal in a coflowing wind of 5 m/s with neutral stability and comparisons are made using short time averaging in both models. The results from JINX and DRIFT to 2% vol/vol centreline concentration are compared in Table 3-1 and good agreement is found.

Table 3-1 Comparison of methane jet predictions between JINX and DRIFT.

	JINX	DRIFT
100 bara distance (m) to 2% vol/vol	123	113
10 bara distance (m) to 2% vol/vol	41	40

3.1.2 Jet in a co-flow

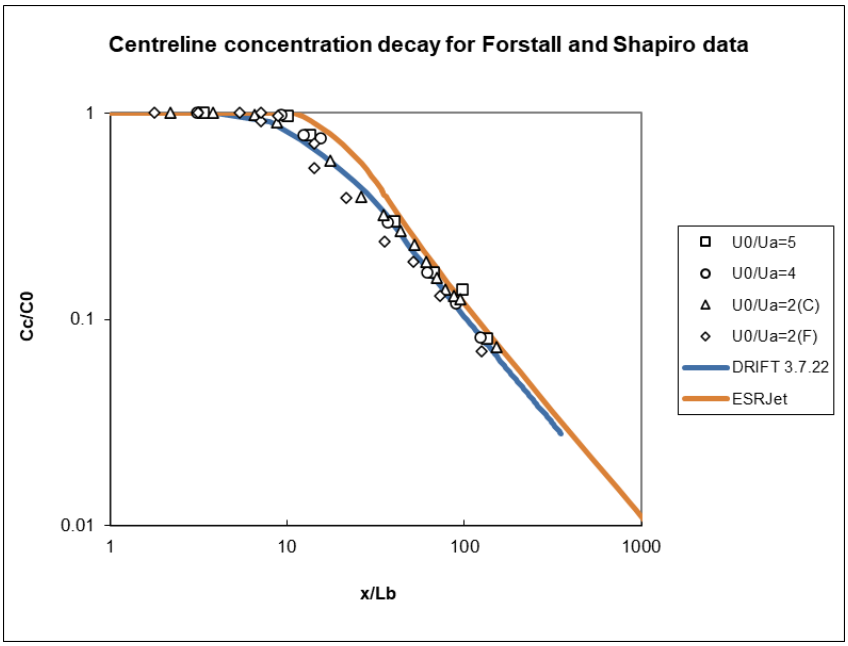

Figure 3-1 Decay of centreline concentration compared with Forstall and Shapiro data [9].

Forstall and Shapiro [9] present data for the decay of centreline concentration in jets of air in a coflowing stream of air. Figure 3-1 shows a comparison of DRIFT 3.7.22 centreline predictions for a jet of air in still air with these data. In Figure 3-1, the centreline concentration, C_c is normalised by the value at the source, C_0 and the distance along the centreline, x is divided by the characteristic length, L_b which is defined in [10] – for a jet in still air it is proportional to the nozzle diameter and for a jet in a co-flow it is based on the conserved excess momentum flux.

DRIFT 3.7.21 and 3.7.22 include an empirical delay for the centreline concentration decay to account for the finite length of the so-called zone of flow establishment over which the lateral profiles evolve from those at the exit (approximated as uniform) to those in the established jet (approximated as Gaussian). The empirical delay is set by tuning to Forstall and Shapiro data and so the comparison shows only that this empirical delay is behaving as intended and additionally confirms that the subsequent jet decay is well represented by the jet entrainment coefficient used in DRIFT. Also shown in Figure 3-1 are the predictions from the jet model ESRJet which is an independently coded implementation of the gas jet model of Cleaver and Edwards [8] on which JINX is also based.

Good agreement is also found for comparison with experimental data for the centreline concentration decay in a methane jet issuing into still air. Unfortunately, the comparison cannot be shown here as the experimental data is confidential.

3.1.3 Jet in a cross-flow

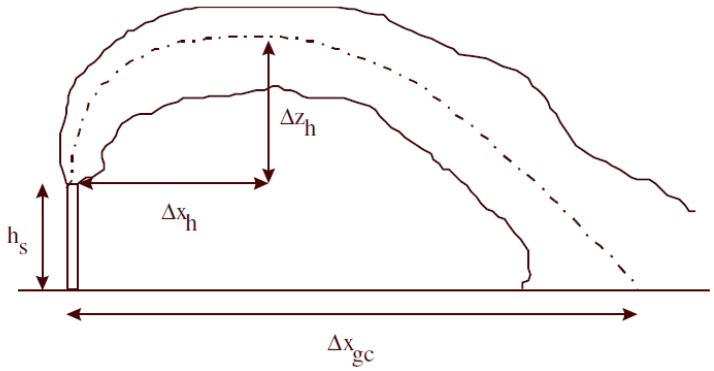

Figure 3-2 Plume rise height and touchdown in the experiments of [11].

Schatzmann et al. [11] conducted wind-tunnel studies on dense jets and plumes from a model stack in both laminar and turbulent crossflows. They presented results for the maximum rise height, concentration and distance at which this occurs, together with the distance to maximum ground-level concentration. The distance definitions are shown schematically in Figure 3-2. Schatzmann et al. varied the momentum and buoyancy flux of the releases as well as the ratio of the jet and crossflow velocities. DRIFT 3.7.22 runs have been undertaken for the turbulent cases only, since they are most relevant to atmospheric dispersion, and the results compared with experimental data are shown in Table 3-2. In this table, Fr_s is the densimetric Froude number of the jet source, D_s is the source diameter, ρ_s/ρ_a is the source density relative to air, U_s/U_a is the source velocity relative to the cross-flow velocity at the source height. The table also includes DRIFT 3.7.19 model predictions. The determination of the maximum rise height and the location of the maximum ground-level concentration are subject to increased uncertainty for very shallow plume trajectories where there is a very slow change in the plume height with distance and in some cases, values are not available from the wind-tunnel measurements. In general, DRIFT compares favourably to these experimental data, especially as there is no tuning of the model parameters to this dataset.

Table 3-2 Comparisons of DRIFT predictions with turbulent cross-flow experiments [11].

run	Fr_s	ρ_s/ρ_a	U_s/U_a	h_s/D_s	$\Delta z_h/D_s$			$\Delta x_h/D_s$			c_h/c_s (%)			$\Delta x_{gc}/D_s$			c_{gc}/c_s (%)		
					3.7.19	3.7.22	expt	3.7.19	3.7.22	expt	3.7.19	3.7.22	expt	3.7.19	3.7.22	expt	3.7.19	3.7.22	expt
1T	30.6	1.56	20.8	12	35	34	42	49	47	39	4.6	4.6	2.6	189	189	252	1.09	1.10	0.91
2T	30.6	1.56	10.4	12	26	26	29	94	97	94	2.7	2.7	1.6	378	378	456	0.32	0.32	0.30
3T	30.6	1.56	5.2	12	19	18	19	194	202	158	1.13	1.1	0.57	535	535	520	0.10	0.10	0.12
4T	766	1.66	33	31.45	164	164	151	25500	26400	3150	0.00085	0.00085	0.016	3145	3145	-	0.009	0.009	-
5T	766	1.66	137	31.45	452	446	401	6270	6415	2520	0.021	0.021	0.088	9308	9308	-	0.005	0.005	-
6T	1313	4.88	33	31.45	282	279	>232	84277	84277	>4095	9.8E-05	9.8E-05	<0.01	5031	5031	-	0.004	0.004	-
7T	1313	4.88	137	31.45	818	805	>650	19245	19182	>4095	0.0033	0.0033	<0.03	16981	16981	-	0.0016	0.0016	-
8T	766	4.88	33	31.45	268	265	>228	25786	25786	>4095	0.0008	0.0008	<0.01	5031	5031	-	0.0037	0.0038	-
9T	766	4.88	137	31.45	679	667	>606	6516	6478	>4095	0.0143	0.0142	<0.029	12579	12579	-	0.0026	0.0027	-
10T	6.23	2.3	2.54	6.69	6.1	6.1	5.4	13	13	15.75	15	15	6.88	75	79	90.55	1.9	1.9	1.49
11T	6.23	2.3	1.27	6.69	4.2	4.2	3.14	26	25	15.75	8.1	8.2	4.65	136	142	150	0.45	0.45	0.33
12T	6.23	2.3	7.51	6.69	8.8	8.8	10.45	3.2	3.1	3.94	35	35	17.83	14	14	24.8	8.0	7.9	3.93
13T	9.06	4.8	2.54	6.69	9.5	9.4	9.13	27	27	31.5	2.8	2.8	2.44	117	117	177.2	0.35	0.35	0.61
14T	6.23	4.8	2.54	6.69	7.5	7.5	7.83	11	11	15.75	5.6	5.6	5.57	54	60	66.93	0.89	0.89	1.66

3.1.4 Two-phase jet

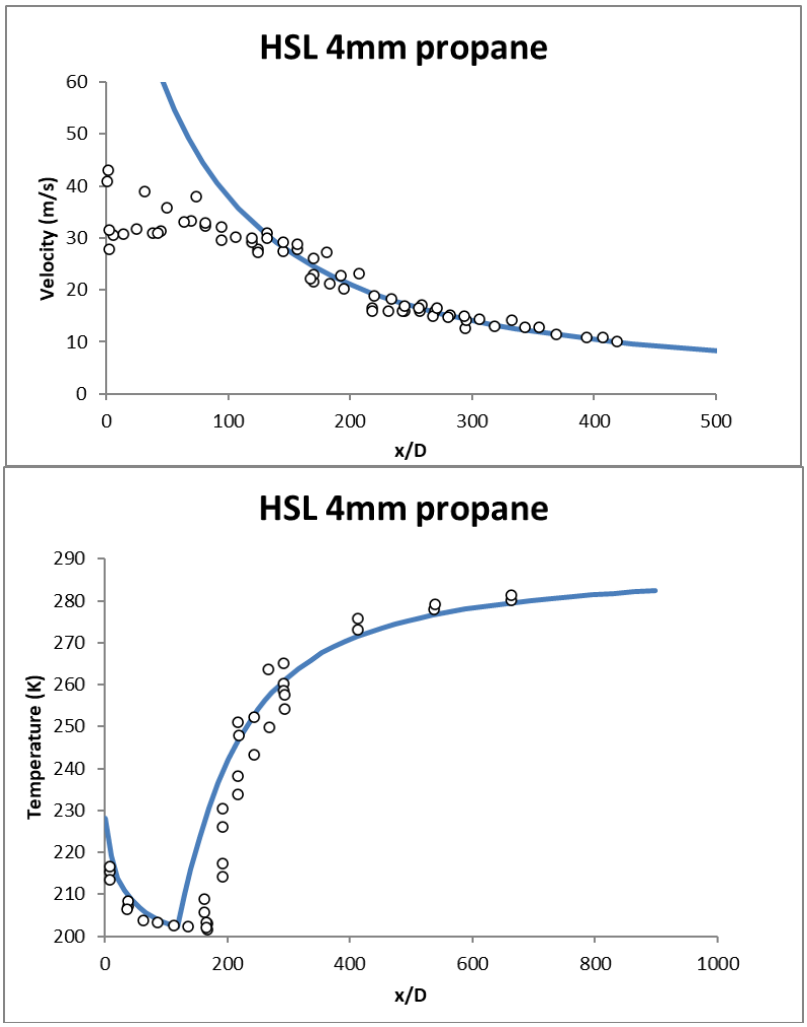

Figure 3-3 DRIFT 3.7.22 comparisons with small-scale two-phase propane jet data.

Coldrick [12] presents comparisons of jet model predictions with temperature and velocity measurements of small-scale two-phase propane jets. One of the models Coldrick compared against was DRIFT 3.7.2. Figure 3-3 compares DRIFT 3.7.22 with these data (release condition and data taken from Tickle et al. (1997) [10]) which confirms that DRIFT 3.7.22 still provides a good representation of these experiments.

3.2 Other field trials

Appendix 1 shows plots of predictions using DRIFT 3.7.22 compared with measurements from selected field trials. These plots show a similar overall level of agreement for DRIFT 3.7.22 with field trail data as seen in previously for versions 3.6.14, 3.7.19 and 3.7.21.

4.0 Conclusions

This document summarises the results of verification testing undertaken by ESR Technology on DRIFT 3.7.22. DRIFT 3.7.22 includes the following improvements over 3.7.19:

- Improvements in the search algorithm used for determining hazard ranges for the case of buoyant clouds and correction of a bug whereby in the specific circumstance of a transient cloud resulting from a buoyant release DRIFT could use zero height, rather than worst case height for calculating concentration contours.

- Improvements to fitting the wall jet data of Davis and Winarto and Rajaratnam, whilst also changing the algorithm for the transition from wall jet to wind-blown jets to give improved agreement with the Desert Tortoise data, particularly at 100m distance where the transition algorithm in DRIFT 3.7.19 previously led to concentration predictions exceeding Model Evaluation Criteria developed for evaluating LNG dispersion models.

- Change to ammonia-water interaction coefficients for improved fit to vapour pressure and heat of mixing over a wider range of conditions.

Apart from the above changes, results from other test cases shows that in general DRIFT 3.7.22 is found to perform similarly to DRIFT 3.7.19.

5.0 References

[1] G. A. Tickle, “Evaluation of Changes in DRIFT Version 3.7.19,” ESR Technology Report ESR/SRM489000/001/Rev 1, 1 April 2025.

[2] M. R. Davis and H. Winarto, “Jet diffusion from a circular nozzle above a solid plane,” *J. Fluid Mech.,* vol. 101, pp. 201-221, 1980.

[3] N. Rajaratnam, Turbulent Jets, Developments in Water Science 5 ed., Elsevier, 1976.

[4] G. A. Tickle, “Evaluation of Changes in DRIFT Version 3.7.21,” ESR Technology Report ESR/SRM4689000/002/Rev 1, 1 April 2025.

[5] M. J. Ivings, S. F. Jagger, C. J. Lea and D. M. Webber, “Evaluating vapor dispersion models for safety analysis of LNG facilities,” The Fire Protection Research Foundation, May 9, 2007.

[6] C. J. Wheatley, “Discharge of ammonia to moist atmospheres - survey of experimental data and model for estimating initial conditions for dispesrion calculations,” UKAEA Report SRD/HSE R410, 1987.

[7] R. Tillner-Roth and D. G. Friend, “A Helmholtz Free Energy Formulation of the Thermodynamics Properties of the Mixture {Water + Ammonia},” *Journal of Physcal and Chemical Reference Data,* vol. 27, 1998.

[8] R. P. Cleaver and P. D. Edwards, “Comparisons of an integral model for predicting the dispersion of a turbulent jet in a cross-flow with experimental data,” *J. Loss Prev. Process Ind.,* vol. 3, pp. 91-96, 1990.

[9] W. Forstall and A. H. Shapiro, “Momentum and mass transfer in coaxial gas jets,” *J. Appl. Mech.,* vol. 17, no. 4, pp. 399-408, Dec 1950.

[10] G. A. Tickle, S. J. Jones, D. Martin, S. A. Ramsdale and D. M. Webber, “Development and validation of two-phase jets,” AEA Technology Report AEAT/1389 Issue 1, March 1997.

[11] M. Schatzmann, W. H. Snyder and R. E. Lawson, “Experiments with heavy gas jets in laminar and turbulent cross-flows,” *Atmos. Environ.,* vol. 27A, no. 7, pp. 1105-1116, 1993.

[12] S. Coldrick, “Modelling small-scale flashing propane jets,” *Chemical Engineering Transactions,* vol. 48, pp. 73-78, 2016.

Appendix 1 Comparisons with selected field trials

A1.1 Thorney Island

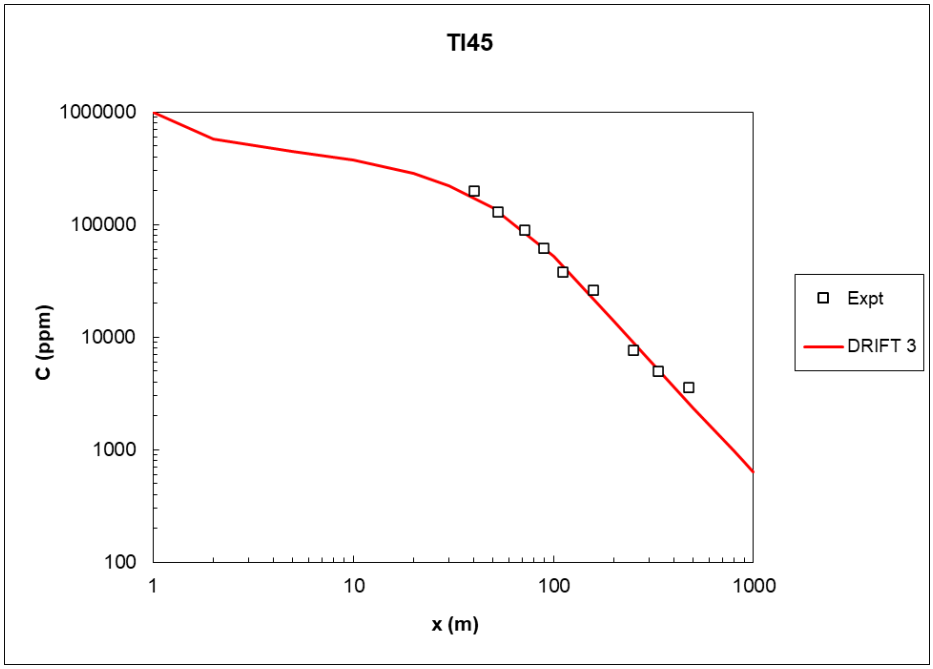

Figure A1- 1 Centreline concentration predictions for Thorney Island Trial 45. DRIFT was originally tuned using this trial.

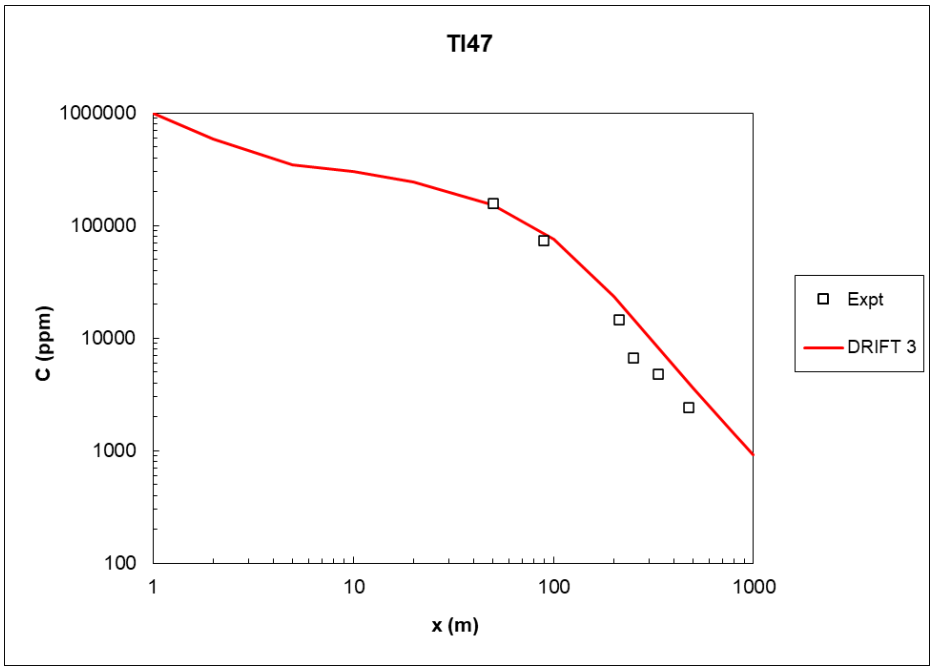

Figure A1- 2 Centreline concentration predictions for Thorney Island Trial 47.

A1.2 Burro

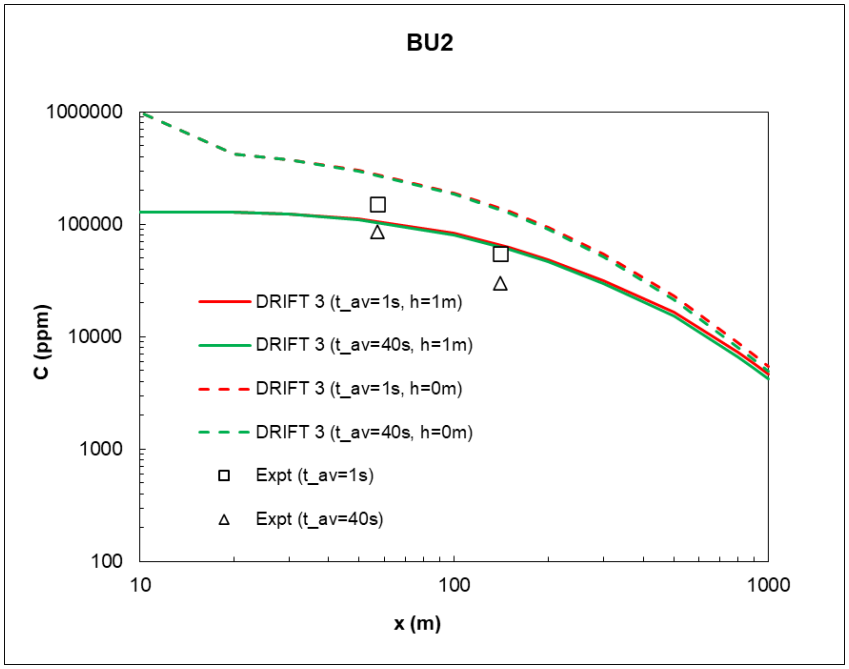

Figure A1- 3 Centreline concentration predictions for Burro Trial 2.

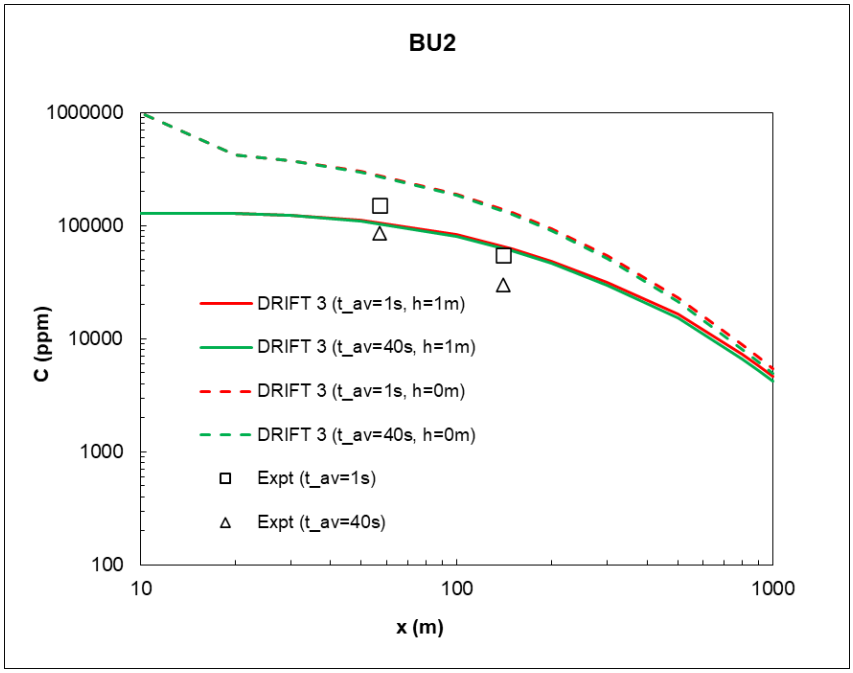

Figure A1- 4 Centreline concentration predictions for Burro Trial 3.

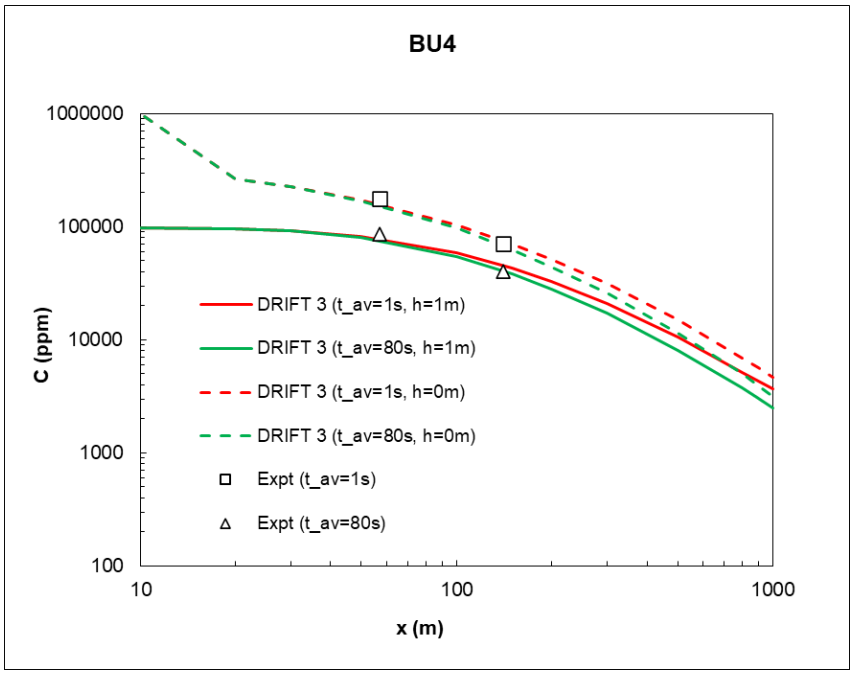

Figure A1- 5 Centreline concentration predictions for Burro Trial 4.

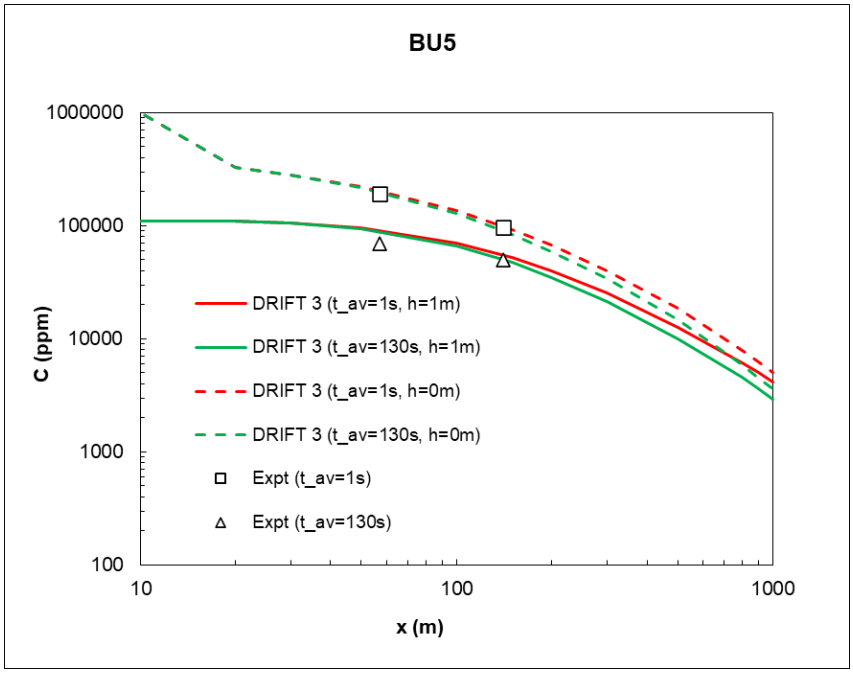

Figure A1- 6 Centreline concentration predictions for Burro Trial 5.

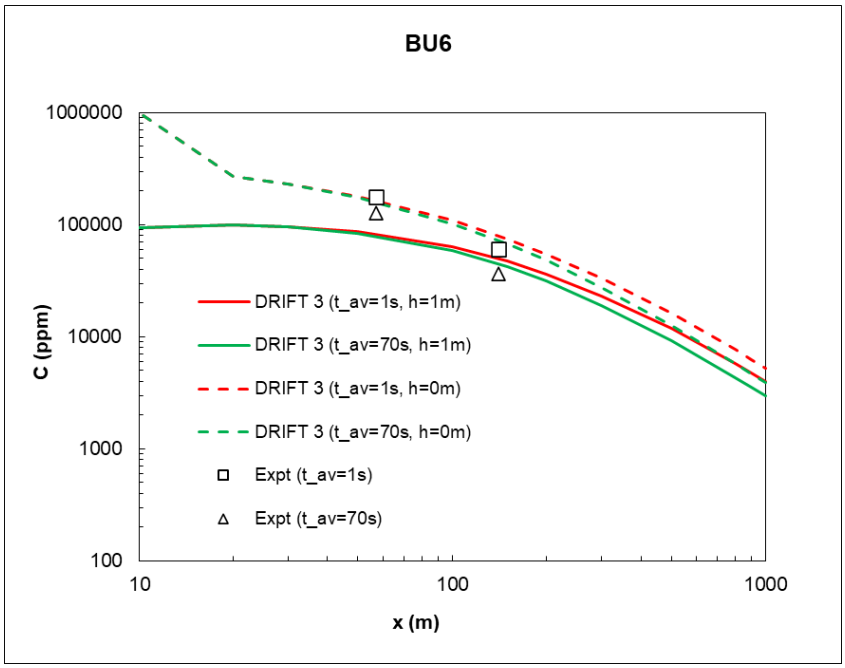

Figure A1- 7 Centreline concentration predictions for Burro Trial 6.

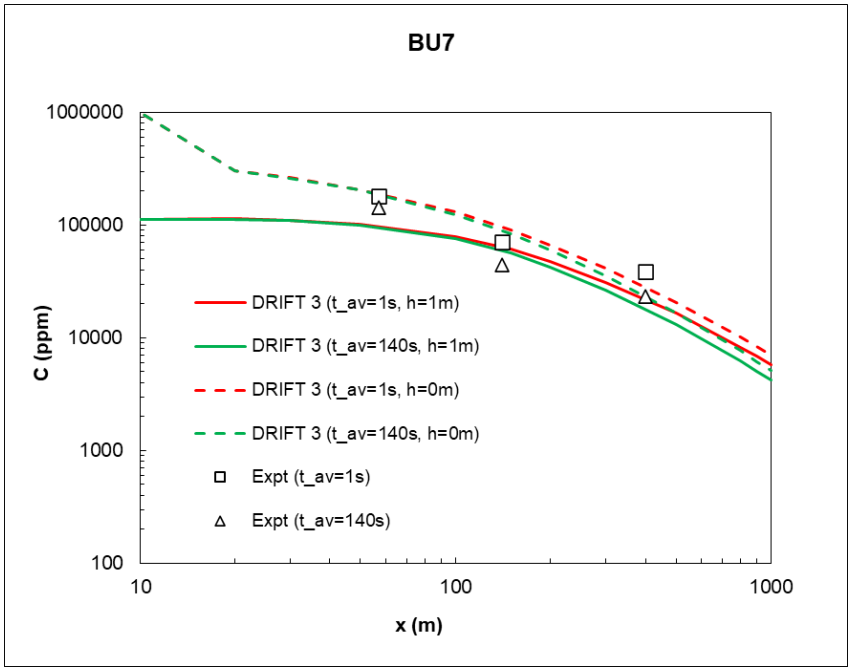

Figure A1- 8 Centreline concentration predictions for Burro Trial 7.

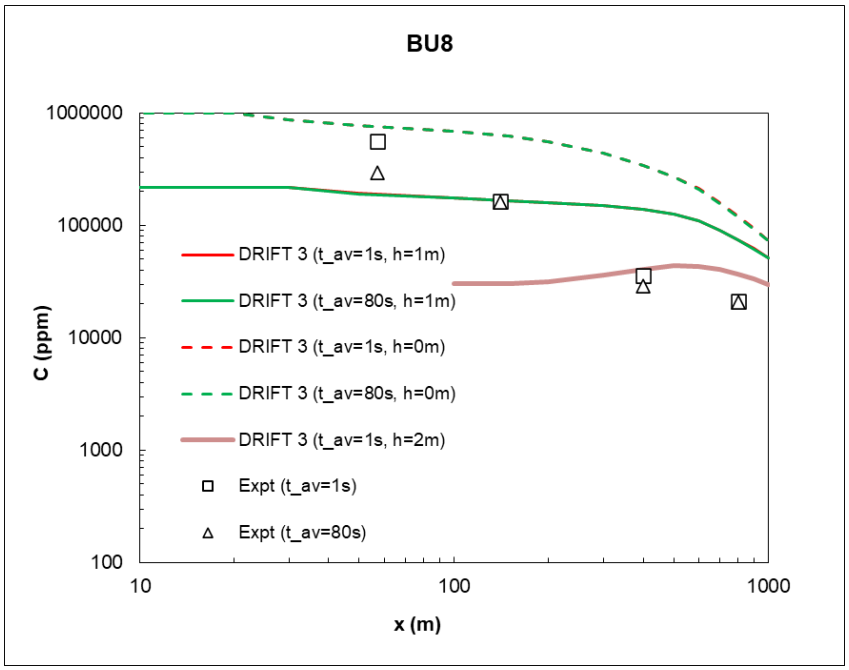

Figure A1- 9 Centreline concentration predictions for Burro Trial 8.

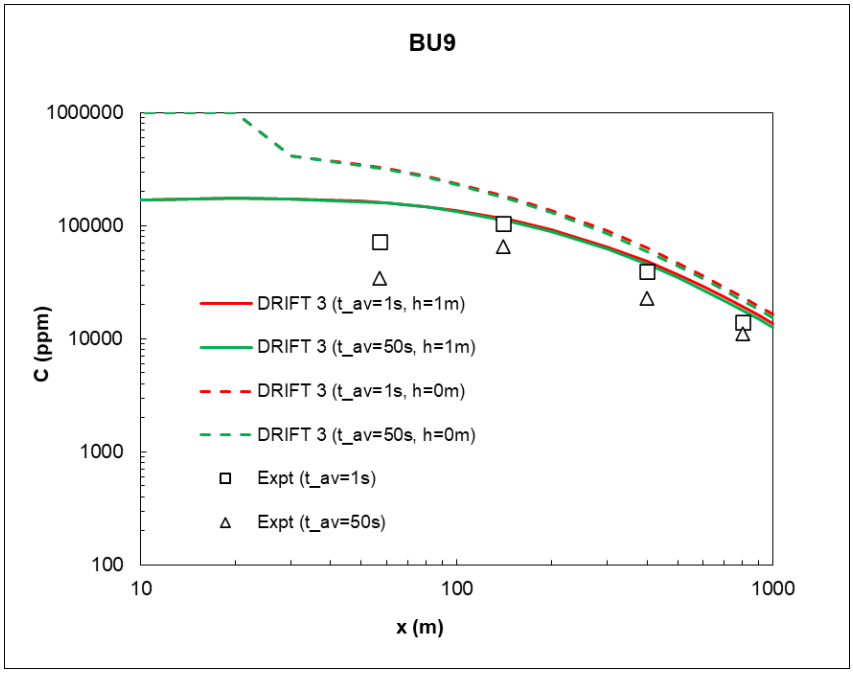

Figure A1- 10 Centreline concentration predictions for Burro Trial 9.

A1.3 Goldfish

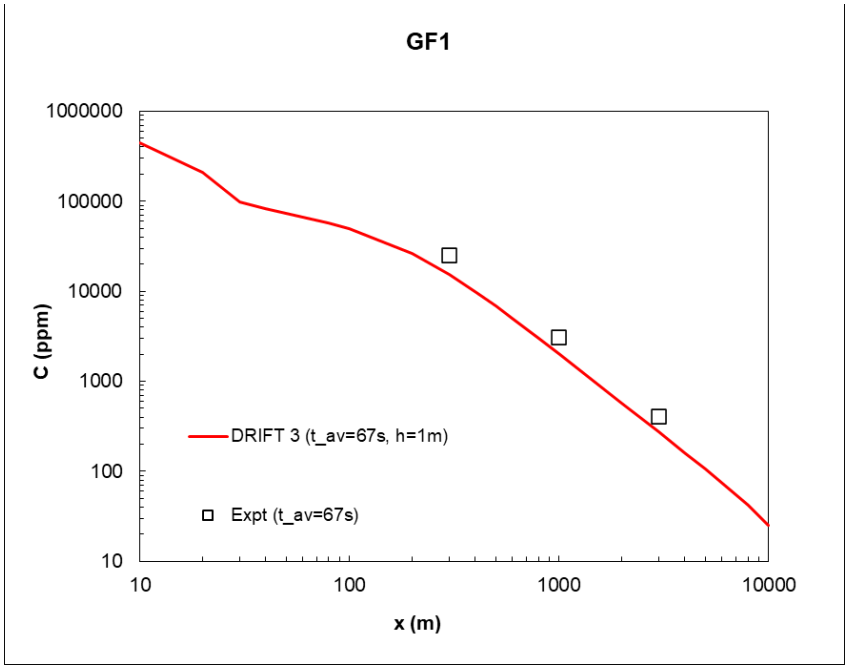

Figure A1- 11 Centreline concentration predictions for Goldfish Trial 1.

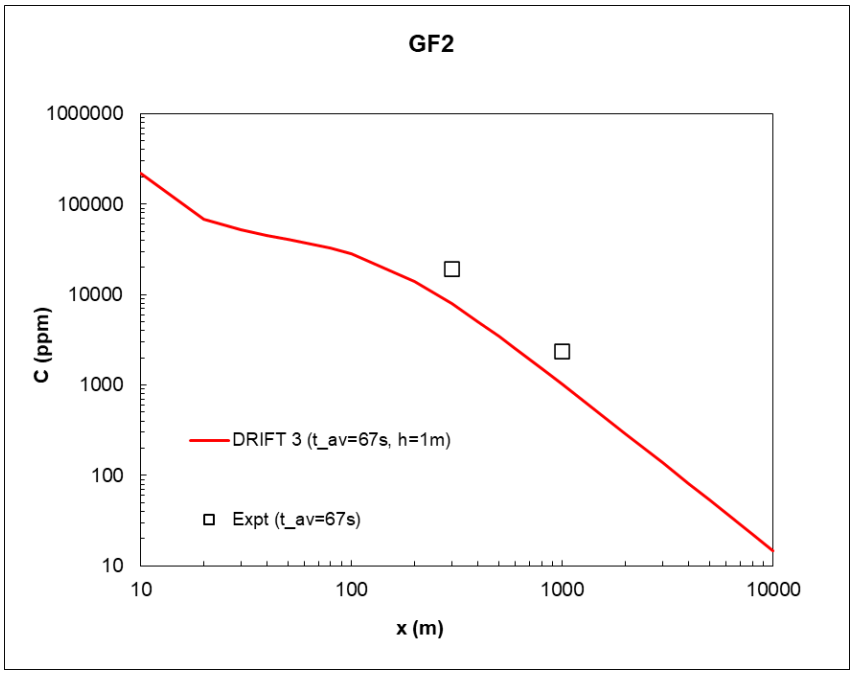

Figure A1- 12 Centreline concentration predictions for Goldfish Trial 2.

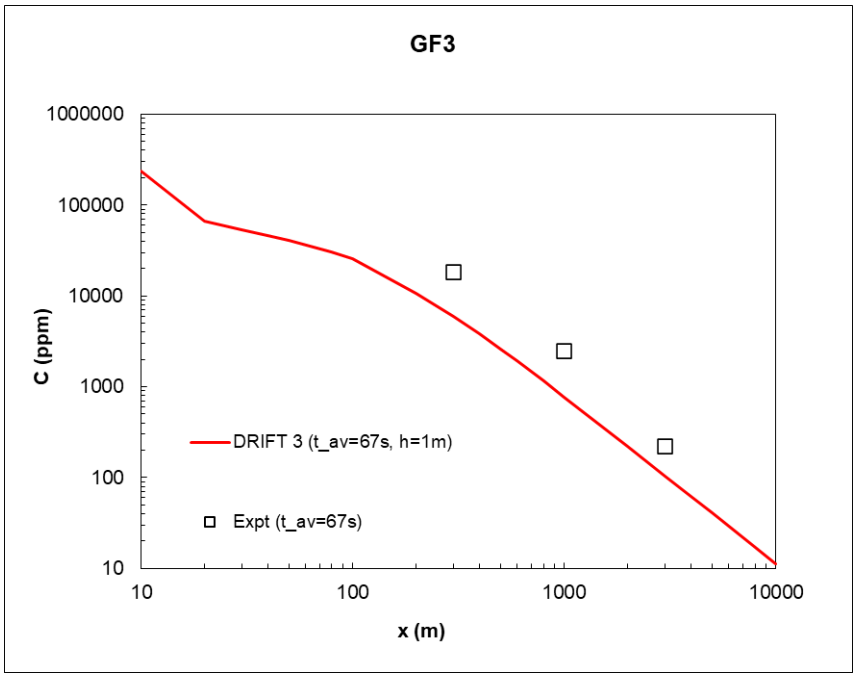

Figure A1- 13 Centreline concentration predictions for Goldfish Trial 3.

A1.4 Prairie Grass

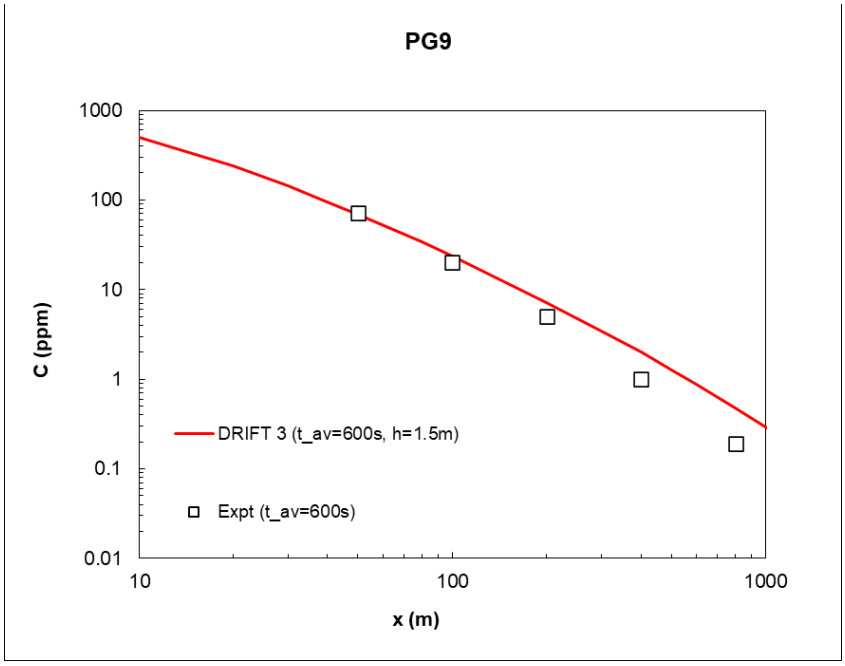

Figure A1- 14 Centreline concentration predictions for Prairie Grass Trial 9.

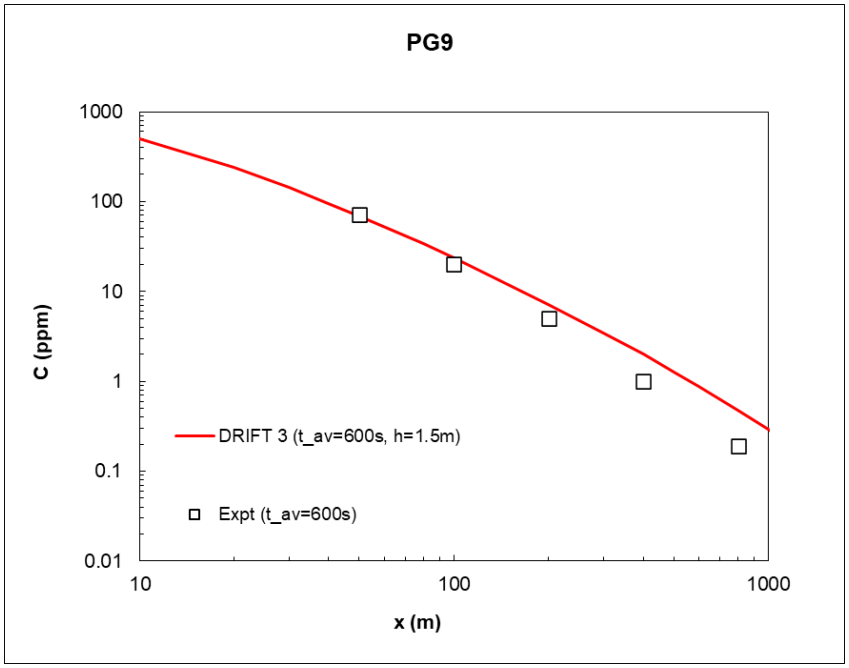

Figure A1- 15 Centreline concentration predictions for Prairie Grass Trial 10.

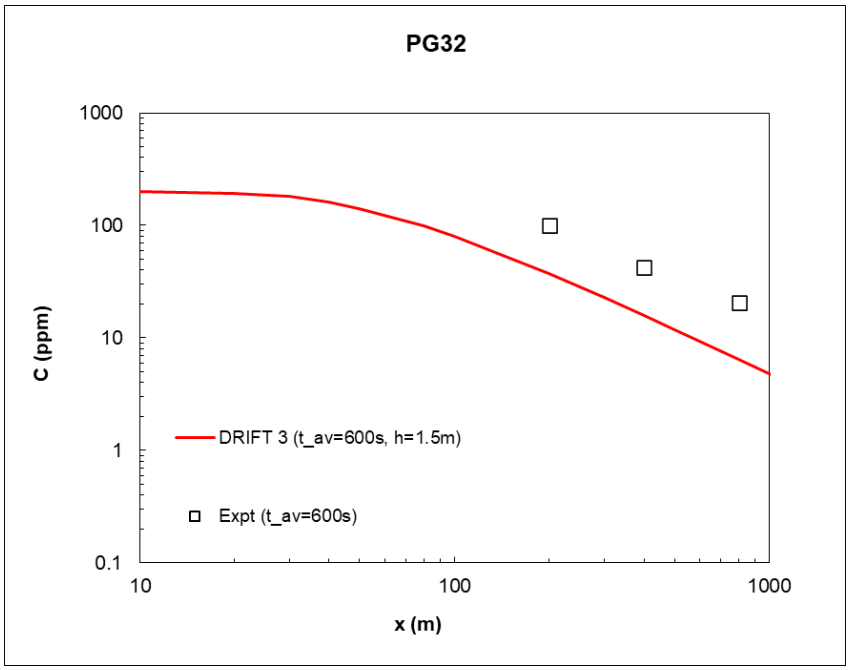

Figure A1- 16 Centreline concentration predictions for Prairie Grass Trial 11.

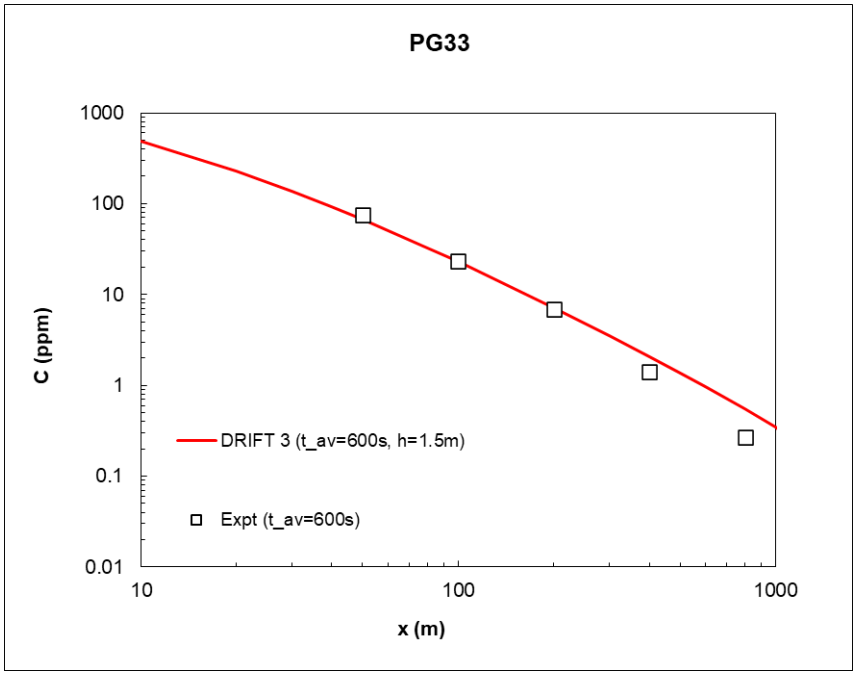

Figure A1- 17 Centreline concentration predictions for Prairie Grass Trial 33.

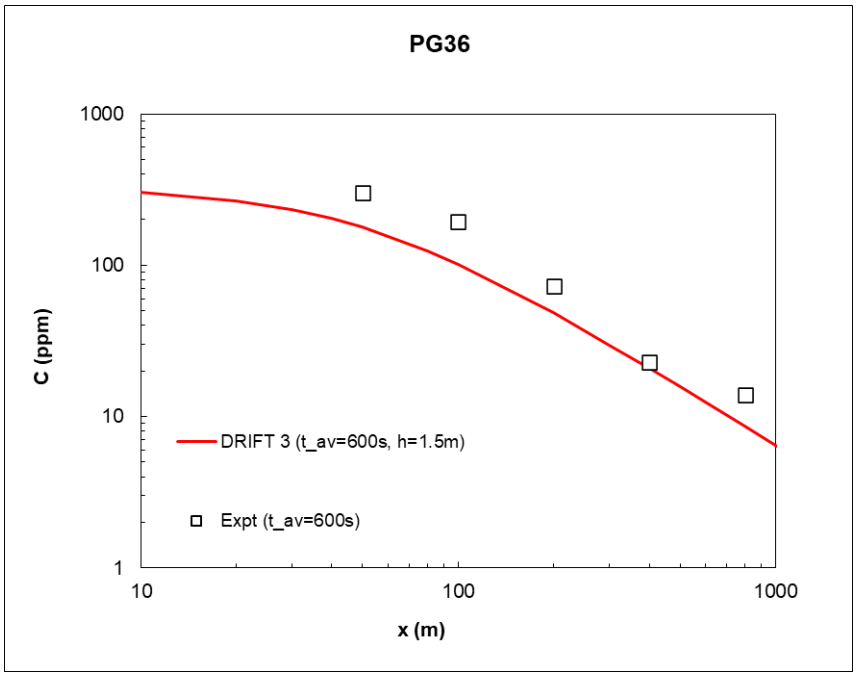

Figure A1- 18 Centreline concentration predictions for Prairie Grass Trial 36.

ESR Technology Ltd, 202 Cavendish Place, Birchwood, Warrington, WA3 6WU, UK
Tel: +44 (0)1925 843400 **Email:** info@esrtechnology.com **Web:** www.esrtechnology.com